
Chapter 8

Fabrication of Dye Sensitized Solar Cell & Its Characterization

8.1 Introduction

The dye sensitized solar cell (DSSC) is one of the promising organic solar cells. It is composed of a dye modified wide bandgap semiconductor electrode, counter electrode and redox electrolyte [1, 2].

The highest efficiency of DSSC has been found to be around 11%. The overall power conversion efficiency of DSSC is affected by many factors including the transmittance and the conductivity of the conducting substrate, properties of TiO₂ film, type of dye or photosensitizer, the electrolyte composition, and the platinum electrode [3-9]. The platinum layer as a counter electrode and Ruthenium (Ru) complex as a photosensitizer (dye) are the expensive parts of DSSC. In the present work, an attempt has been made to replace these expensive parts with low cost and easily available material. Carbon is coated on conducting plate to use as a counter electrode instead of platinum and natural dye extracted from pomegranate juice was used instead of the Ruthenium complex.

The most commonly used dye is a Ruthenium(Ru) complex. Rubipyridyl complexes have been studied intensively as a photosensitizer for homogeneous photocatalytic reactions and dye sensitization systems because of its long life times and long term chemical stability of oxidized Ru (III) [10]. Different Ru complexes having carboxylic groups as anchors to adsorb on to the semiconductor surface have been studied [11, 12]. The *cis*-bis(4,4'-dicarboxy-2,2'-bipyridine)dithiocyanato ruthenium (II) (RuL₂(NCS)₂ complex), which is referred to as N3 dye or red dye can absorb over a wide range of the visible regions from 400 to 650 nm. The trithiocyanato 4, 4'4''-tricarboxy-2,2':6',2''-terpyridine ruthenium (II) referred to as

black dye ($\text{RuL}'(\text{NCS})_3$ complex), absorbs in the near IR region up to 900 nm. There are three parameters which photosensitizer should possess [13].

- (1) The sensitizer should have extremely high broad band absorption in UV, Visible, and IR region.
- (2) The transfer of electron between the photo-excited sensitizer and photoanode must be rapid and energetically favorable.
- (3) The photosensitizer should have high photo stability. The material must be capable of many oxidation-reduction cycles without decomposition.

As Ru metal is rare and expensive, the synthetic complexes of Ru metal based are very expensive to use as a photosensitizer. Alternatively organic dyes can also be utilized as a photosensitizer. Organic dyes have been explained in Chapter 2. A ZnO electrode sensitized by organic dyes including rose Bengal, fluorescein, and rhodamine B was studied by Gerischer and Tributsch [14, 15]. Organic dyes are generally extracted from plants. The different colors of plants, flowers, fruits and leafs are results of production, interaction and breakdown of three classes of substances: porphyrins, carotenoids, and flavonoids. Organic dyes have several advantages as photosensitizers:

- (1) They have a variety of structures for molecular design,
- (2) They are cheaper than metal complexes,
- (3) They have large absorption coefficients.
- (4) They are obtained from renewable sources.
- (5) Practically no or mild reactions are involved in their preparation.
- (6) Natural dyes cause no disposal problems, as they are biodegradable.

In the present work, natural dye extracted from pomegranate juice has been used. Pomegranate contains anthocyanins. Anthocyanins belong to flavonoid group and are responsible for most red, blue, and purple colors in plants, flowers and leaves. The binding of carbonyl and hydroxyl groups to the surface of porous TiO₂ film is the advantage of anthocyanin which causes electron transfer from the anthocyanin molecule to conduction band of TiO₂ [16].

8.2 Fabrication of Dye Sensitized Solar cell

8.2.1 Preparation of the TiO₂-ZrO₂ Electrode

The film of electrode material i.e. TiO₂-ZrO₂ is usually prepared by one of the two methods: (1) Doctor Blade Technique, (2) Screen Printing. In the present work, the film has been prepared by doctor blade technique. The powder was grinded in an agate mortar with dilute acetic acid for 1 hour. A non-ionic surfactant such as Triton X -100 is added to prepare mono disperses paste. The obtained paste was coated on ITO glass plate by glass rod, using adhesive tapes (3M) as spacers. The films were dried in air at room temperature. Then the coated conducting glass plate was sintered at 450 °C for 30 min. This film was used as working or photo electrode.

8.2.2 Dye Fixation onto the TiO₂-ZrO₂ Film

After preparation of TiO₂-ZrO₂ films, the dye is adsorbed onto the TiO₂-ZrO₂ surface. In the present work, anthocyanin dye present in pomegranate juice is used as a sensitizer, as mentioned above. The films are immersed into the dye solution (pomegranate juice) followed by storage at room temperature for 18 h in dark, so that it is properly adsorbed on the film. This treatment produces intense coloration of

the film. Before being used, the film is washed with isopropanol to remove excess non adsorbed dyes inside the porous TiO₂-ZrO₂ film.

8.2.3 Redox Electrolyte Preparation

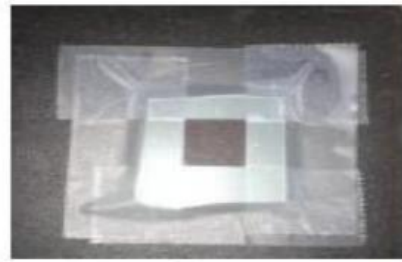
The electrolyte used in DSSC is Iodine solution, which contains I⁻/I₃⁻ redox ions. These ions mediate electrons between the photo electrode and the counter electrode. Br⁻/Br₂ and hydroquinone have been also used as redox electrolyte for DSSC but the iodine redox electrolyte gives the best performance [17, 18]. In the present work, KI based electrolyte was used. 0.127 gm Iodine (I₂) was dissolved in 10 ml of ethylene glycol. 0.83 gm potassium iodide (KI) was mixed in this solution and stirred for few minutes and stored in a dark.

8.2.4 Preparation of Counter Electrode

The reduction process between dye cations and I⁻ ions produces tri-iodide I₃⁻. Tri-iodide ion reduces to I⁻ at the counter electrode and for this the counter electrode must have high electro catalytic activity. The most commonly used catalytic material is platinum [19]. Replacement of expensive platinum counter electrode is challenge to ensure a low charge transfer resistance and high exchange current densities. Carbon based materials are also applied as the material for counter electrode but the efficiencies are found to be lower [20, 21]. In the present work graphite is used for counter electrode. A thin layer of graphite is coated on conducting plate by pencil. This plate works as a counter electrode.

8.2.5 Assembling the Cell and Cell Performance

After preparing photo electrode and counter electrode, a sandwich type DSSC is assembled. A film of polyethylene is placed at the sides on dye adsorbed $\text{TiO}_2\text{-ZrO}_2$ photo electrodes which work as a spacer and provide insulation between two electrodes. After that two electrodes (photo electrode and counter electrode) are fixed together by binder clips. The redox electrolyte comprising of iodide/tri-iodide containing solution is introduced into the gap between the counter electrode and the working or photo electrode by the capillary force. Figure 8.1 shows step by step fabrication process of dye sensitized solar cell.



Scotch tape as a spacer is put on the conducting side of ITO glass



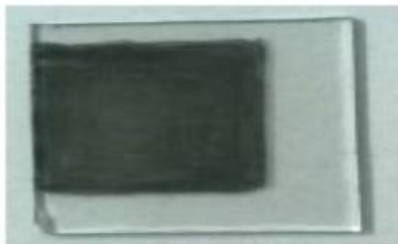
TiO₂-ZrO₂ paste is applied and dispersed with a glass rod on the same side of the ITO glass.



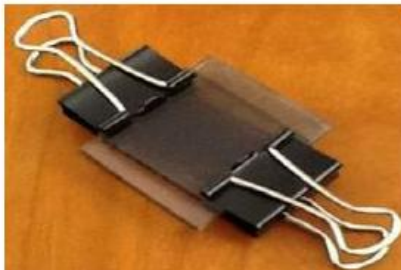
The coated conducting glass plate is sintered at 450°C for 30 min.



This electrode is immersed in pomegranate juice for 18 h.



Graphite is coated with a dark pencil on the conducting surface of another ITO glass as a counter electrode.



Both the electrodes are put together and iodine solution is introduced to complete the process.

Figure 8.1. Fabrication process of Dye Sensitized Solar Cell

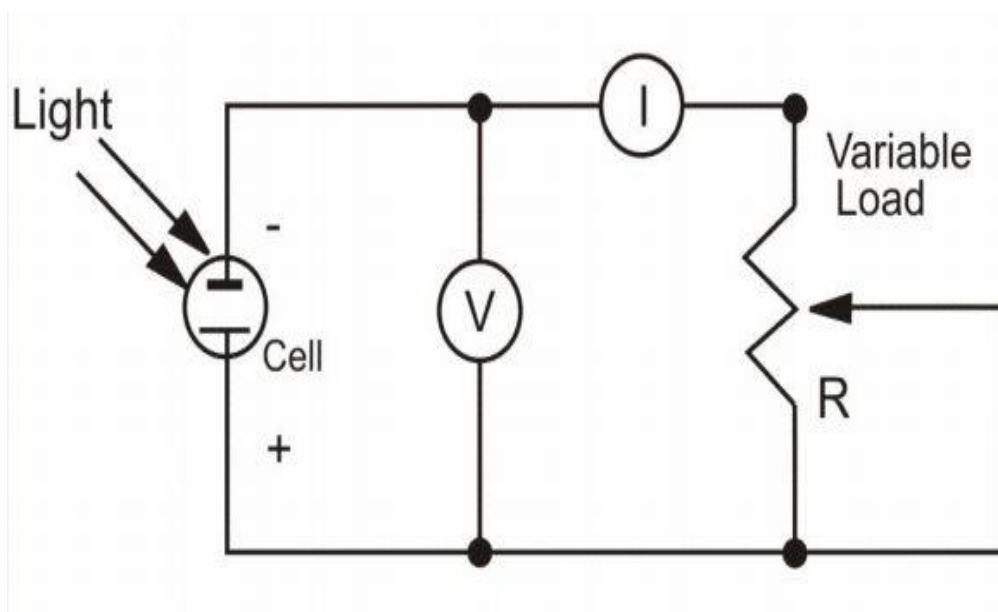


Figure 8.2. Circuit diagram for I-V characteristic measurements

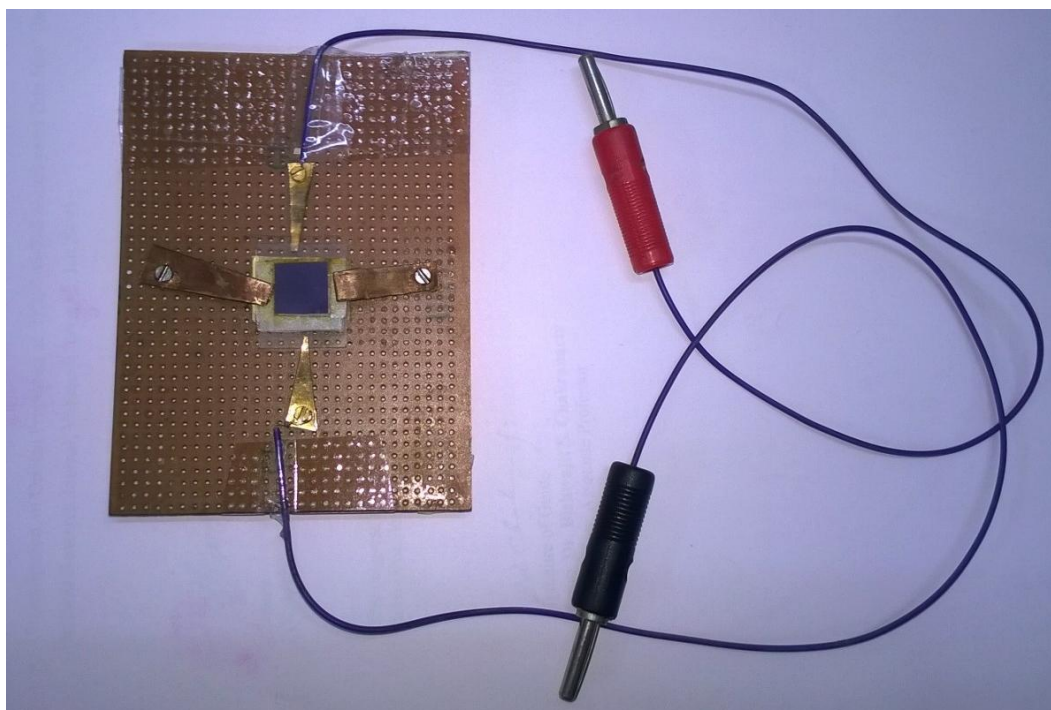


Figure 8.3. Contact arrangements for Dye Sensitized Solar Cell

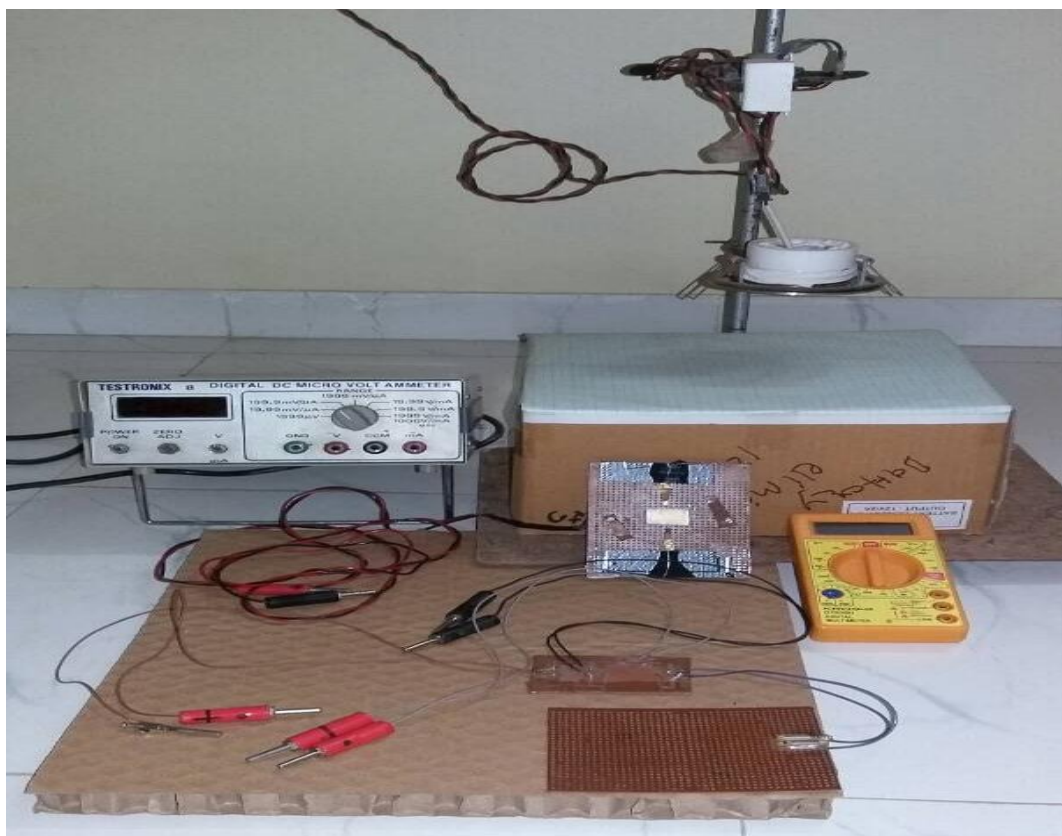


Figure 8.4 Set up for the efficiency measurements of Dye Sensitized Solar Cell

A simple I-V measurement system was devised to measure open circuit voltage and short circuit current of the fabricated DSSC's. The I-V characteristics of the cells were measured with a fixed load under illumination. For illumination, white LED of 3 W was used. Figure 8.2 shows the circuit diagram for measuring I-V characteristics. For measuring current and voltage, a Testronix make digital DC micro voltmeter and micro ammeter was used, while a $100\text{K}\Omega$ resistor was used as a load. For these measurements, an assembly was prepared which can hold the prepared solar cell with contact arrangements. To minimize series resistance the copper contacts were coated with gold. The contact arrangements and setup for efficiency measurements are shown in figure 8.3 and 8.4 respectively.

8.3 Photovoltaic performance

8.3.1 Parameters to be measured

The performance of DSSC is evaluated by measuring the parameters such as short circuit current (I_{SC}) and open circuit voltage (V_{OC}) under illumination. The IV curve is used to find I_{max} and V_{max} , the product of which gives maximum power i.e. P_{max} . The conversion efficiency η , of the solar cell can be obtained by calculating the fill factor FF , the power density P , the photocurrent density at short circuit J_{SC} and the open circuit photo voltage V_{OC} .

Short Circuit Current (I_{SC})

The short circuit current corresponds to short circuit condition and it is calculated when the voltage is 0. For an ideal cell, I_{SC} is the maximum current or total current produced in the solar cell by photon excitation.

$$I_{SC} = I \text{ (at } V = 0) \quad [1]$$

Open Circuit Voltage (V_{OC})

Open circuit voltage occurs when there is no current passing through the cell. V_{OC} is also the maximum voltage difference across the cell.

$$V_{OC} = V \text{ (at } I = 0) \quad [2]$$

Maximum Power (P_{max})

Maximum power produced by cell can be easily calculated from I-V curve.

The power density of the cell is given by the product of photocurrent density at short circuit ($J = I_{sc}/\text{Surface area of the cell}$) and voltage (V).

$$P = JV \quad [3]$$

Fill Factor

The fill factor is the ratio of the maximum obtainable power to theoretical power. When the fill factor value is close to 1, it can be considered as an efficient cell. It is given by the following relation.

$$FF = \frac{J_{max} \times V_{max}}{J_{sc} V_{oc}} \quad [4]$$

Power Conversion Efficiency

The power conversion efficiency of dye sensitized solar cells was calculated by the relation given below.

$$\eta = \frac{J_{sc} \times V_{oc} \times FF}{P_{in}} \quad [5]$$

Where P_{in} = Input power (power of light source)

8.3.2 Resistance

One of the major factor which can affect the overall power conversion efficiency of DSSC is the resistance of the solar cell. There can be two types of resistance affecting the efficiency. The resistance can be determined from the I-V characteristic of DSSC as shown in figure 8.5 [22].

1) Series resistance:

The series resistance results from the sheet resistance of TCO, the resistance due to improper ionic diffusion in electrolyte, resistance of contacts and the resistance at the interface of counter electrode and electrolyte are the elements responsible for series resistance of DSSC. Ideally series resistance would be zero. Series resistance can be estimated by the slope near the point V_{oc} on the IV curve.

2) Shunt Resistance:

Shunt resistance is caused by leakage current through the cell due to impurities or defects in the manufacturing process. Ideally shunt resistance is infinite so that no additional current path exists. The lower shunt also leads to a smaller open circuit voltage. Shunt resistance can be calculated by the inverse of slope near the point, short circuit current I_{sc} on the IV curve.

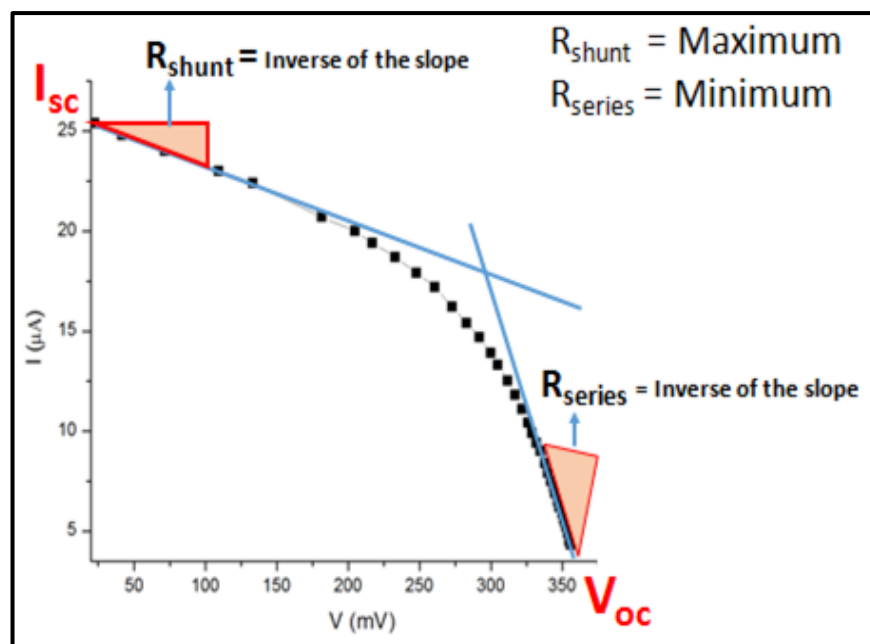


Figure 8.5 Determination of series and shunt resistance from I-V curve

8.3.3 Recombination

The efficiency of DSSC also depends on how fast and efficiently the electrons can be collected from conduction band of $\text{TiO}_2\text{-ZrO}_2$ by the working electrode. The electrons in conduction band of $\text{TiO}_2\text{-ZrO}_2$ can either recombine with oxidized dye or redox electrolyte. The loss of photo generated electron produced by interfacial charge recombination is one of the key problems of DSSC. Figure 8.6 shows electron transfer process in DSSC [23]. There are two possible recombination mechanisms: (a) recombination between the injected electron and the oxidized dye molecule, (b) recombination between the injected electron and triiodide in the electrolyte.

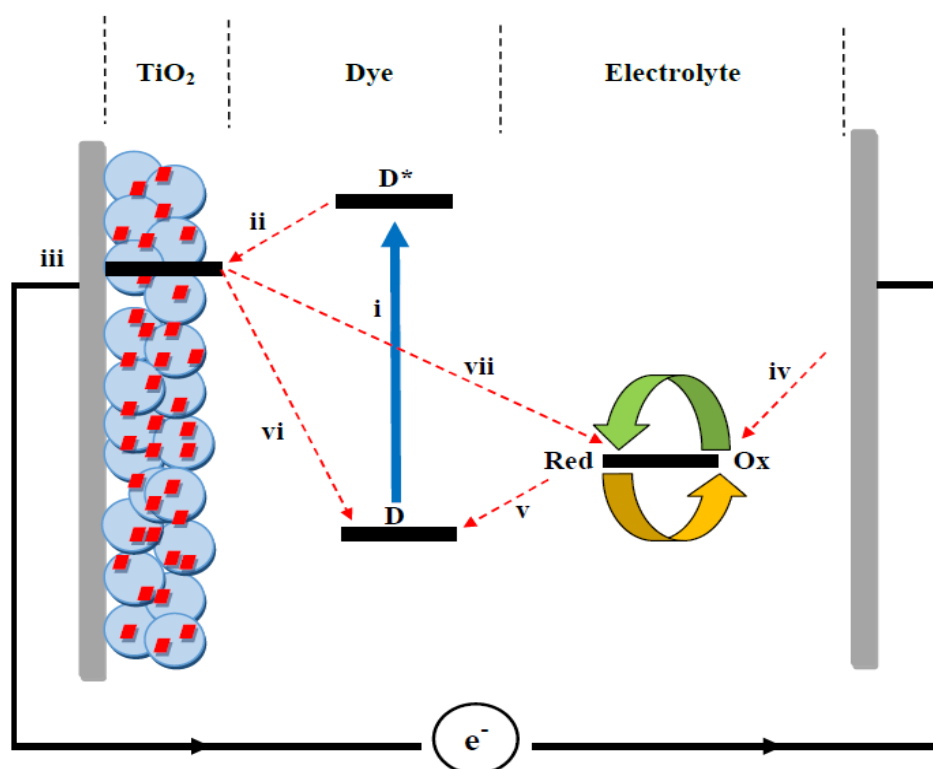


Figure 8.6 Electron transfer process in DSSC with the time scales given below.

- (i) Dye electronic excitation (**femtoseconds**).
- (ii) Charge injection to semiconductor conduction band (**150 picoseconds**).
- (iii) Diffusion of electron from conduction band of TiO_2 to FTO (**100 μs**).
- (iv) Reduction of electrolyte at counter electrode.
- (v) Dye regeneration (transfer of electron from electrolyte to dye) (**1 μs**).
- (vi) Charge recombination from conduction band of TiO_2 to dye (**3 μs**).
- (vii) Charge recombination from conduction band of TiO_2 to electrolyte (**1 ms**).

Recombination is considered to be one of the major reasons for lowering of efficiency. One of the major focuses of research in the field of DSSC today is to address this problem.

8.4 Performance of Dye Sensitized Solar Cell fabricated using un-doped TiO₂-ZrO₂ composites

Dye sensitized solar cell using TiO₂-ZrO₂ mixed oxide were fabricated using the method mentioned above. To check reproducibility of efficiency of solar cells prepared using these mixed oxides, several cells for the same material were prepared and performance of all of them were measured. The best performance has been reported.

Apart from physiochemical and structural properties of material there are several other factors which can affect the efficiency of dye sensitized solar cell, like thickness of the film, porosity of the film, area of the film, particle size of material, uniformity of the film and amount of surfactant used to prepare the cell. These parameters are very difficult to control during fabrication process as the film is prepared by doctor blade technique.

An attempt was made to maintain the uniformity of the paste by grinding it for same time interval and with same amount of material as well as surfactant for each cell. All other parameters like type of dye, dye adsorption time, amount of electrolyte solution, etc. was fixed. In order to examine the performance, the current-voltage i. e. I-V characteristics of DSSC have been measured.

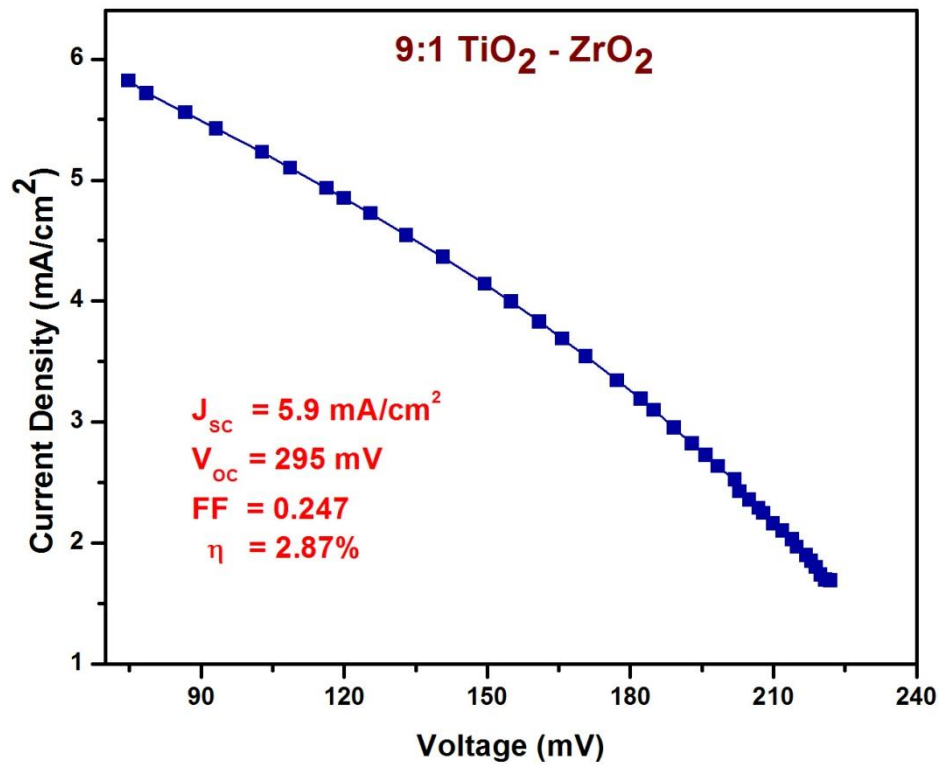


Figure 8.7 I-V curve of DSSC prepared using 9:1 TiO₂-ZrO₂

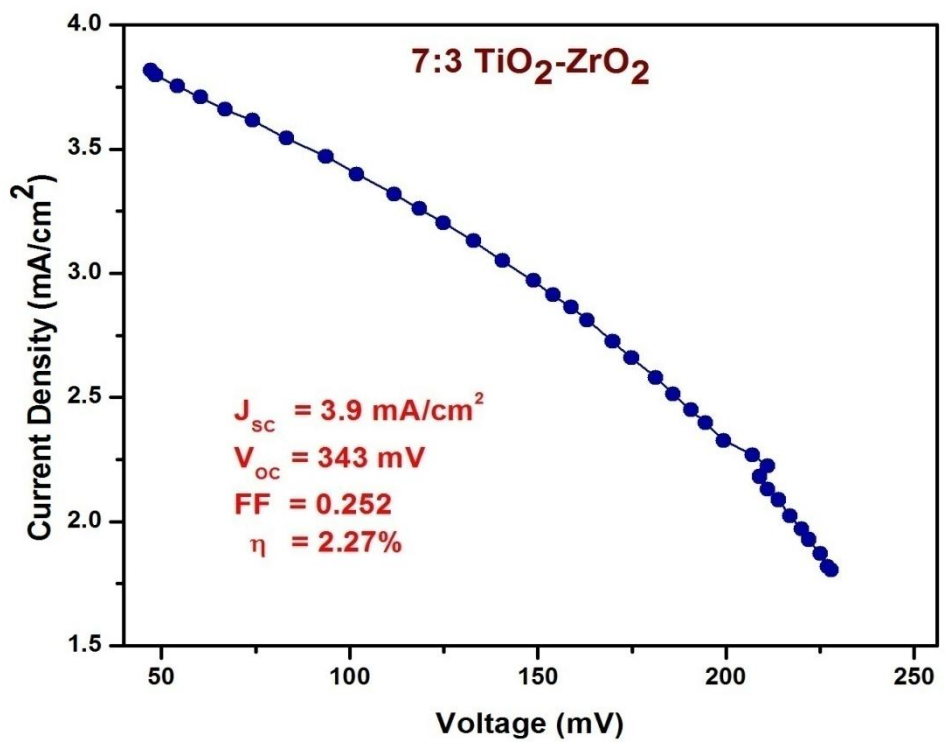


Figure 8.8 I-V curve of DSSC prepared using 7:3 TiO₂-ZrO₂

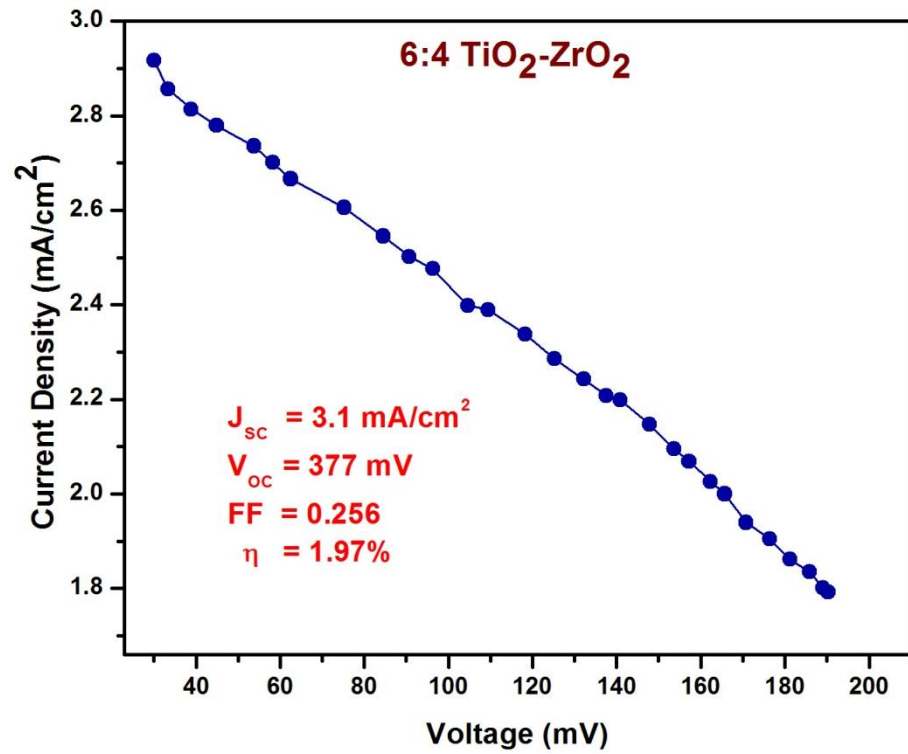


Figure 8.9 I-V curve of DSSC prepared using 6:4 TiO₂-ZrO₂

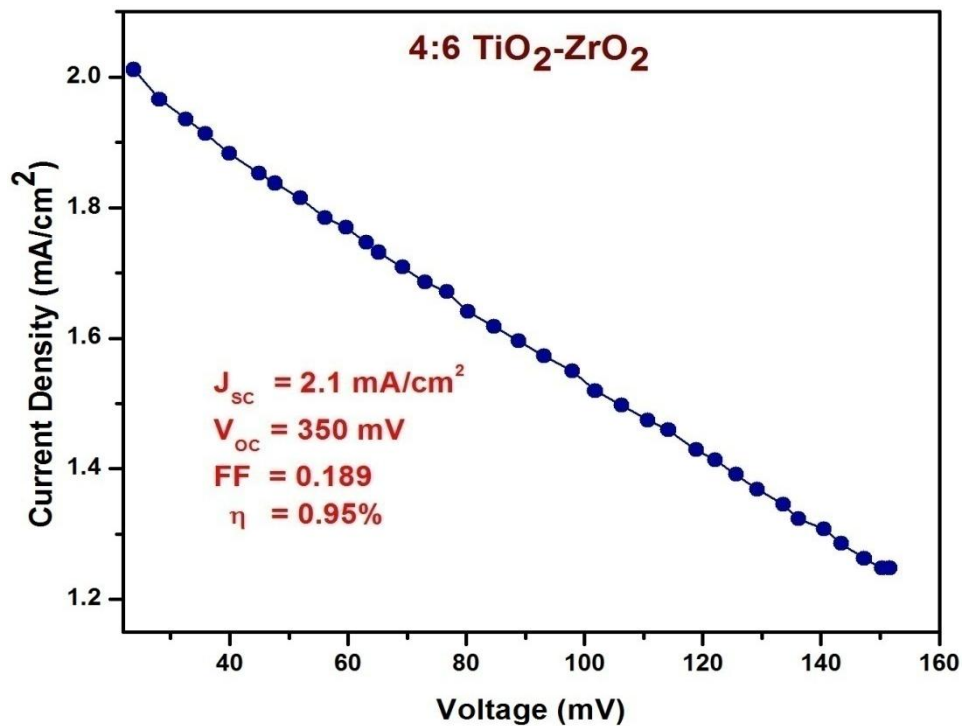


Figure 8.10 I-V curve of DSSC prepared using 4:6 TiO₂-ZrO₂

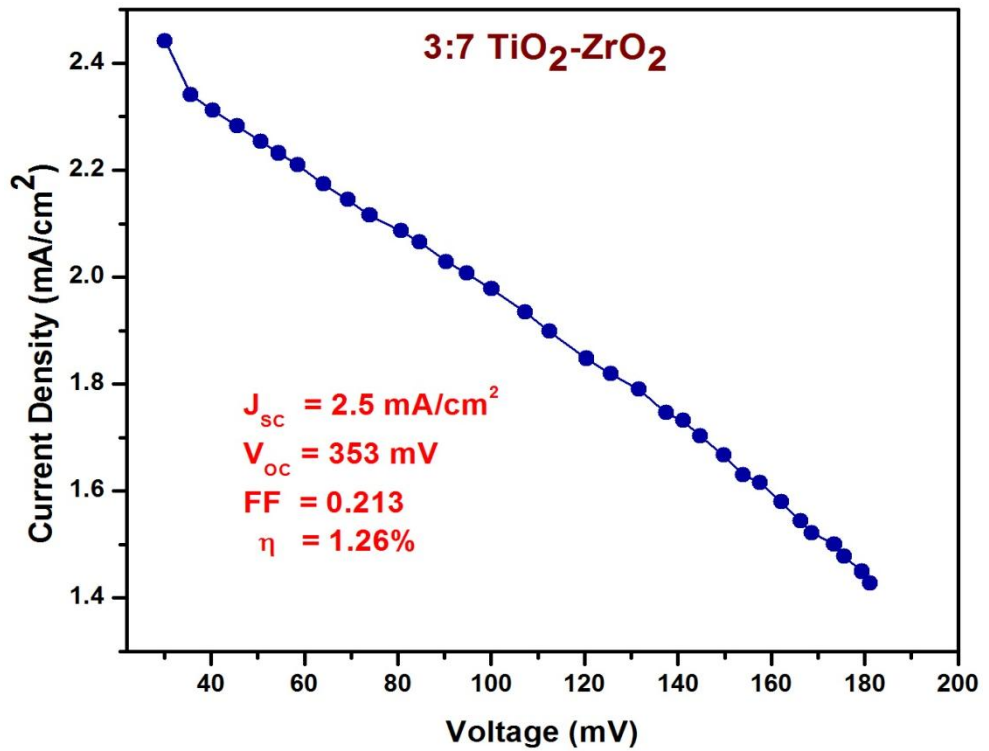


Figure 8.11 I-V curve of DSSC prepared using 3:7 TiO₂-ZrO₂

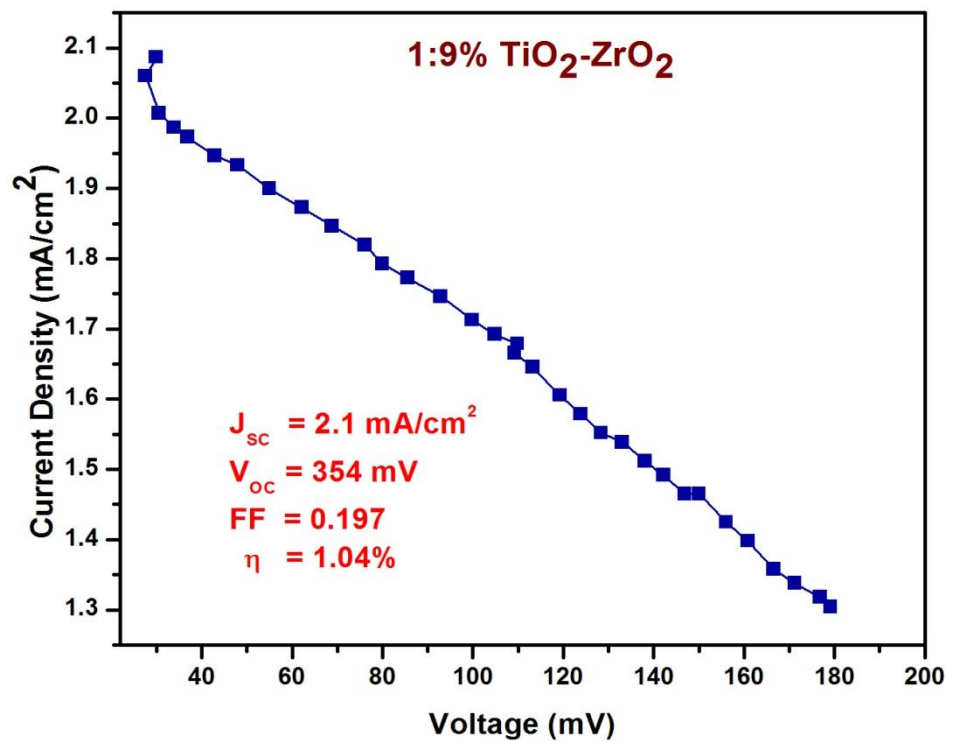


Figure 8.12 I-V curve of DSSC prepared using 1:9 TiO₂-ZrO₂

Table 8.1 Efficiency parameters of DSSC prepared using TiO₂-ZrO₂ samples

Sample	Area Cm ²	R _{shunt} (Ω)	R _{series} (Ω)	J _{SC} mA/cm ²	V _{OC} mV	FF	η %	Overall Anatase Content
9:1 TiO₂-ZrO₂	1.44	0.033	0.017	5.9	295	0.247	2.87	45.35%
7:3 TiO₂-ZrO₂	1.38	0.098	0.036	3.9	343	0.252	2.27	43.42%
6:4 TiO₂-ZrO₂	1.15	-	-	3.1	377	0.256	1.97	29.22%
4:6 TiO₂-ZrO₂	1.32	-	-	2.1	350	0.189	0.95	21.15%
3:7 TiO₂-ZrO₂	1.38	-	-	2.5	353	0.213	1.26	12.59%
1:9 TiO₂-ZrO₂	1.49	-	-	2.1	354	0.197	1.04	3.59%

I-V curves of DSSC prepared using TiO₂-ZrO₂ samples are given in figure 8.7 to 8.12. The first two cells i.e. for samples 9:1 TiO₂-ZrO₂ and 7:3 TiO₂-ZrO₂, conventional I-V curves were recorded. For rest of the cells, the I-V curve shows straight line graph. The straight line nature of curves indicates presence of high resistance in these cells. Because of straight line, the values of shunt and series resistance could not be calculated.

Table 8.1 shows the comparison of efficiency parameters of solar cells with one of the structural parameters of the material i. e. the Anatase content of TiO₂-ZrO₂ mixed oxides. The efficiency is seen to be gradually decreasing.

It has been observed that the efficiency of the cells decrease with increasing content of ZrO₂ and decreasing content of Anatase type TiO₂.

ZrO₂ is high bandgap material and therefore, the electrical resistance of the material will be on the higher side. The series resistance of solar cell increases with higher content of ZrO₂, which can be one of the reasons for decrease in efficiency.

Apart from electrical resistance of the material, there are several other structural parameters which affect the efficiency of solar cell. One of them is the amount of material in Anatase phase of TiO₂. TiO₂ exists in three different phases Anatase, Rutile and Brookite. Among these phases, Anatase is the most favorable phase for solar cell application. Thus for better performance of solar cell material should have high content of Anatase phase.

The gradual decrease in efficiency of the cells can be also attributed to the Anatase content, which offers higher electron transport than Rutile phase [24, 25]. As the Anatase content decreases in the successive samples, the efficiency decreases.

Higher short circuit current density is observed in DSSC prepared using 9:1 TiO₂-ZrO₂ and 7:3 TiO₂-ZrO₂ samples. This can be attributed to a larger amount of dye adsorbed on the surface and better conductivity of the photo electrode i.e. the mixed oxide sample. Usually, J_{SC} is directly related to an amount of dye adsorbed on the photo electrode surface.

8.5 Performance of Dye Sensitized Solar Cells fabricated using metal doped TiO₂-ZrO₂

DSSC's prepared using un-doped TiO₂-ZrO₂ in the ratio of 9:1 and 7:3 give efficiency of more than 2%. To improve the efficiency of solar cell, the structural and optical properties of the photo electrode material need to be modified. For better efficiency, the material should have small particle size so that high amount of dye can be adsorbed on the surface. Material should be porous so that dye can be stored in the porosity of the material. Porosity also increases the surface area for adsorption. To absorb in wider region of solar spectrum, the material should have low bandgap with high absorption coefficient.

In the present work, TiO₂-ZrO₂ mixed oxides have been doped with different metal to alter its structural and optical properties. The incorporation of metal into TiO₂-ZrO₂ affects the specific surface area, light scattering, electron transport rate, and also the porosity. Three types of metal dopants were taken. These are transition metals, alkaline earth metals and rare earth metals. The performance of dye sensitized solar cells prepared with these metal doped TiO₂-ZrO₂ are discussed here.

The I-V curve for dye sensitized solar cells prepared using different metal doped TiO₂-ZrO₂ samples are shown in figure 8.13 to figure 8.26. The parameters are summarized in table 8.2 in increasing order of efficiency.

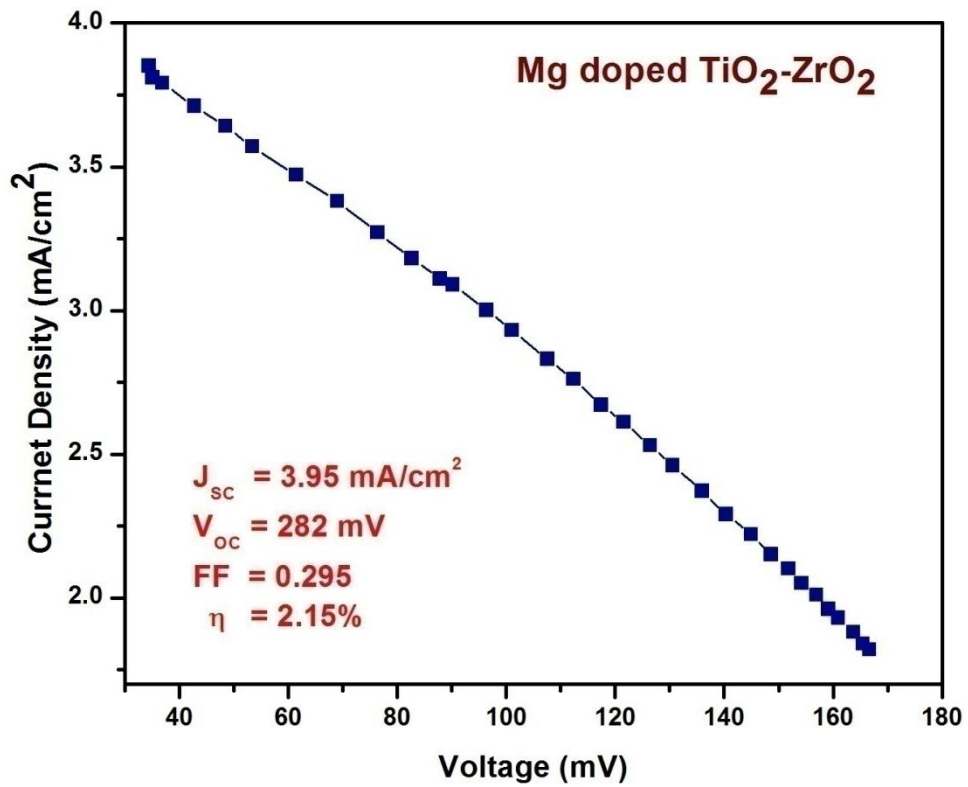


Figure 8.13: I-V curve of DSSC prepared using Magnesium doped TiO₂-ZrO₂

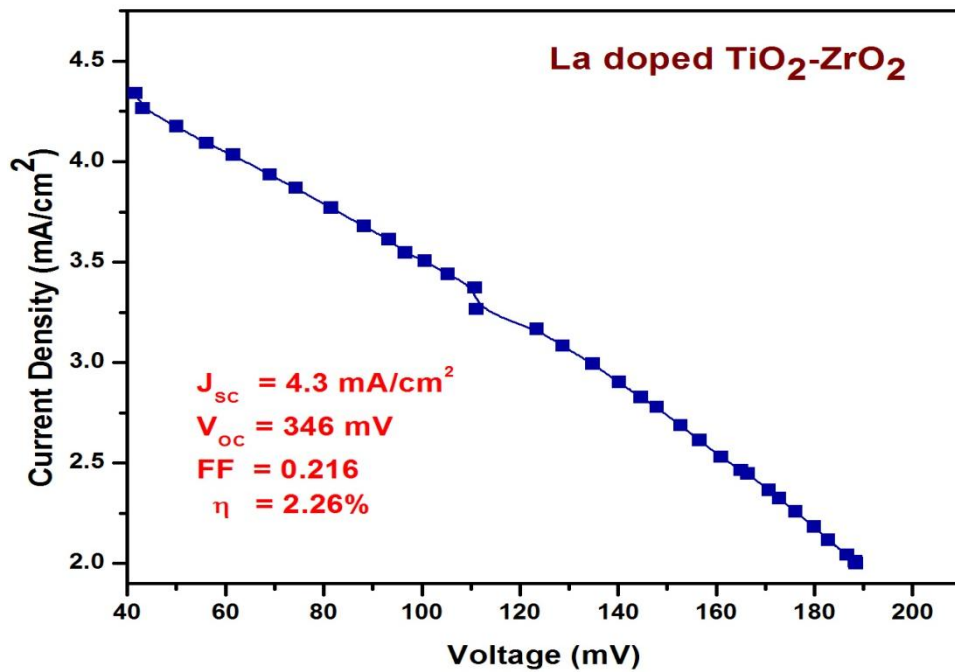


Figure 8.14: I-V curve of DSSC prepared using Lanthanum doped TiO₂-ZrO₂

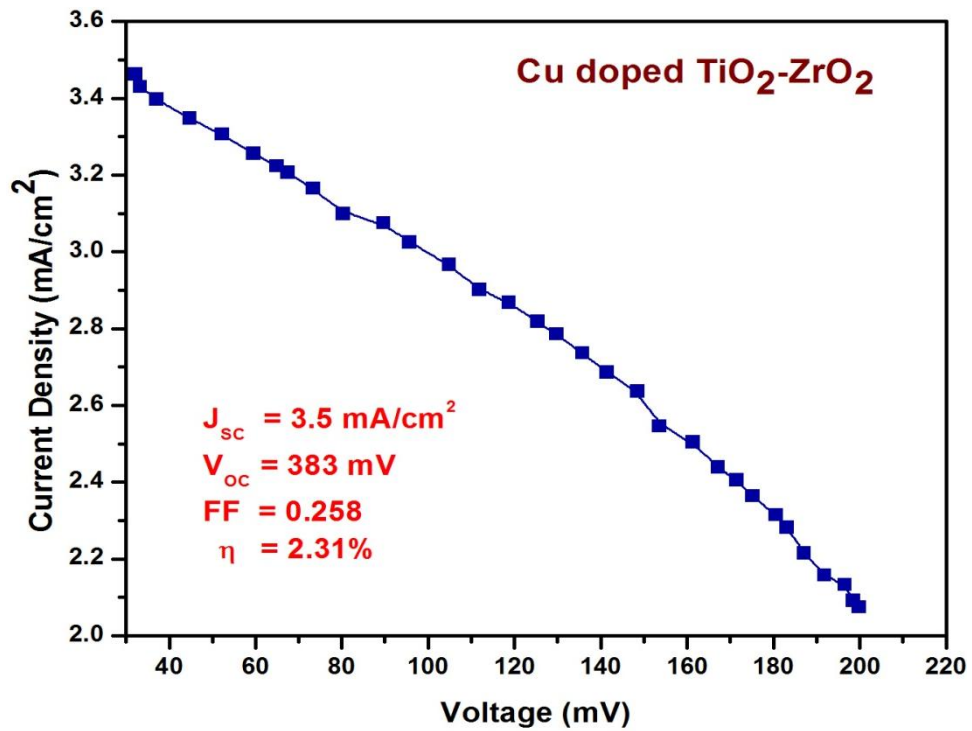


Figure 8.15: I-V curve of DSSC prepared using Copper doped TiO₂-ZrO₂

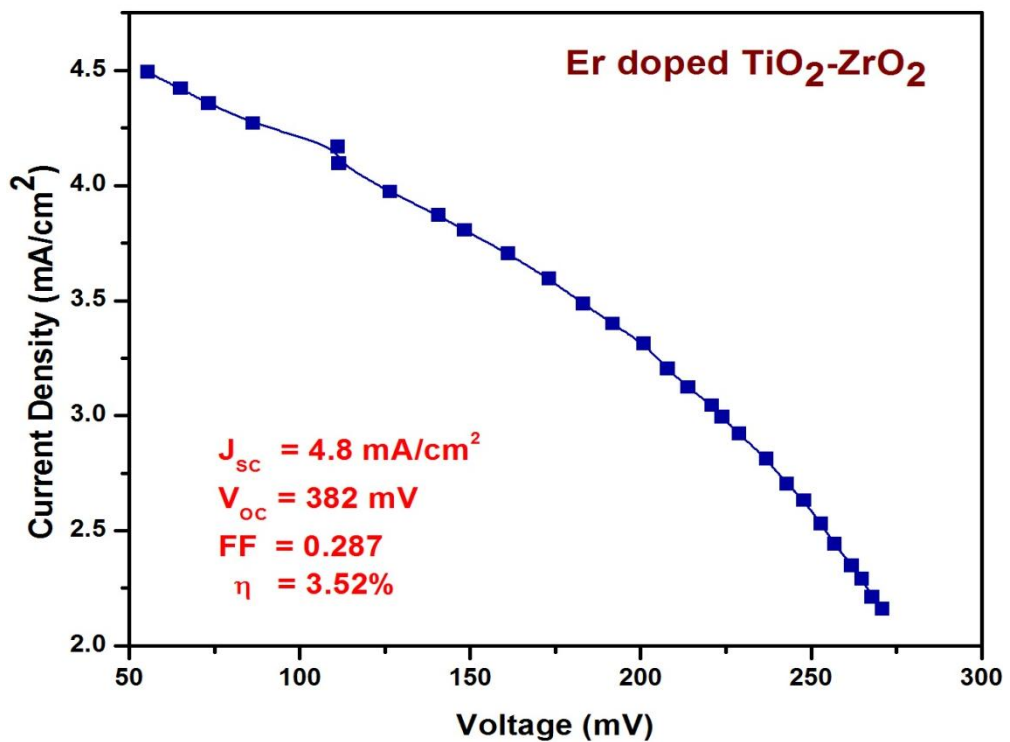


Figure 8.16: I-V curve of DSSC prepared using Erbium doped TiO₂-ZrO₂

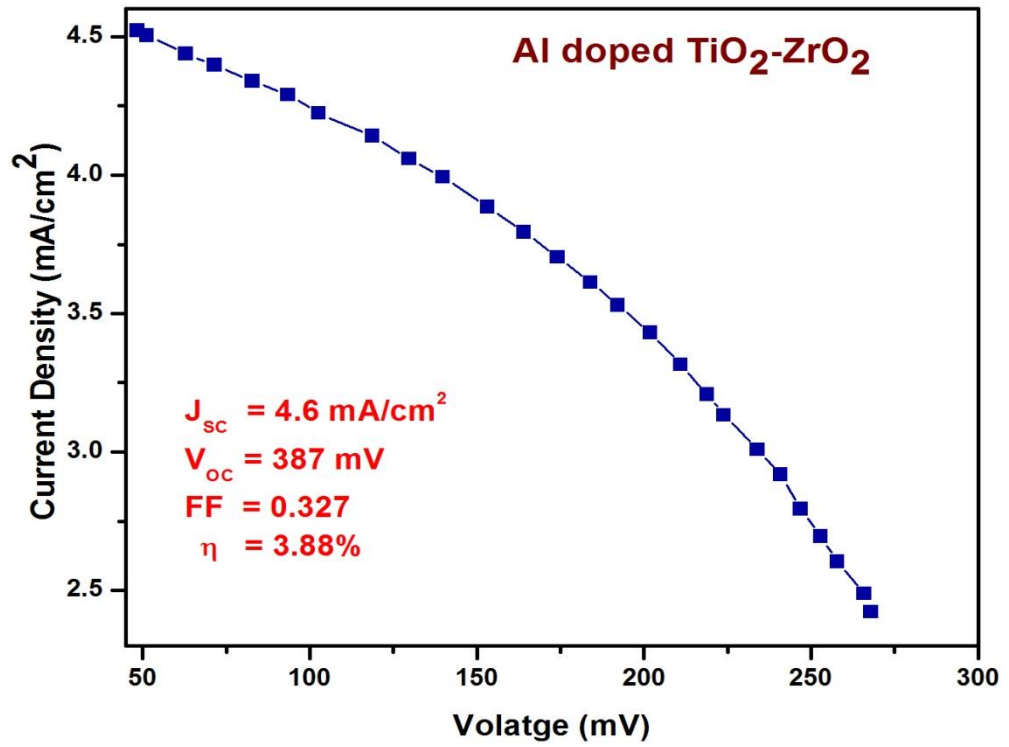


Figure 8.17: I-V curve of DSSC prepared using Aluminium doped TiO₂-ZrO₂

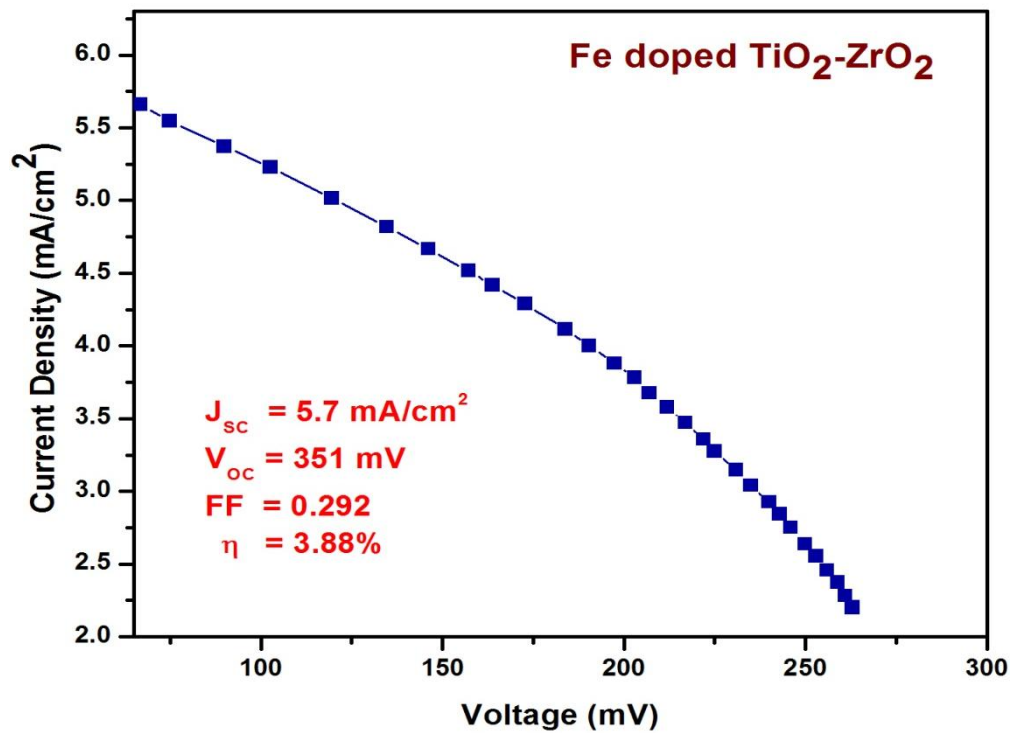


Figure 8.18: I-V curve of DSSC prepared using Iron doped TiO₂-ZrO₂

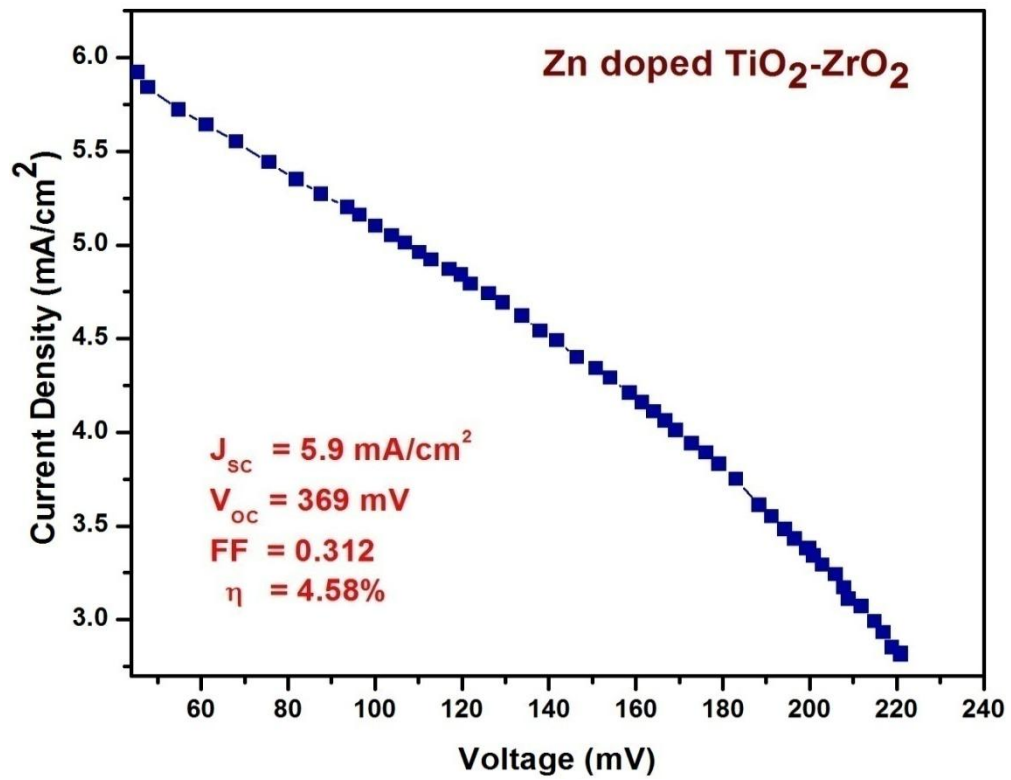


Figure 8.19 I-V curve of DSSC prepared using Zinc doped TiO₂-ZrO₂

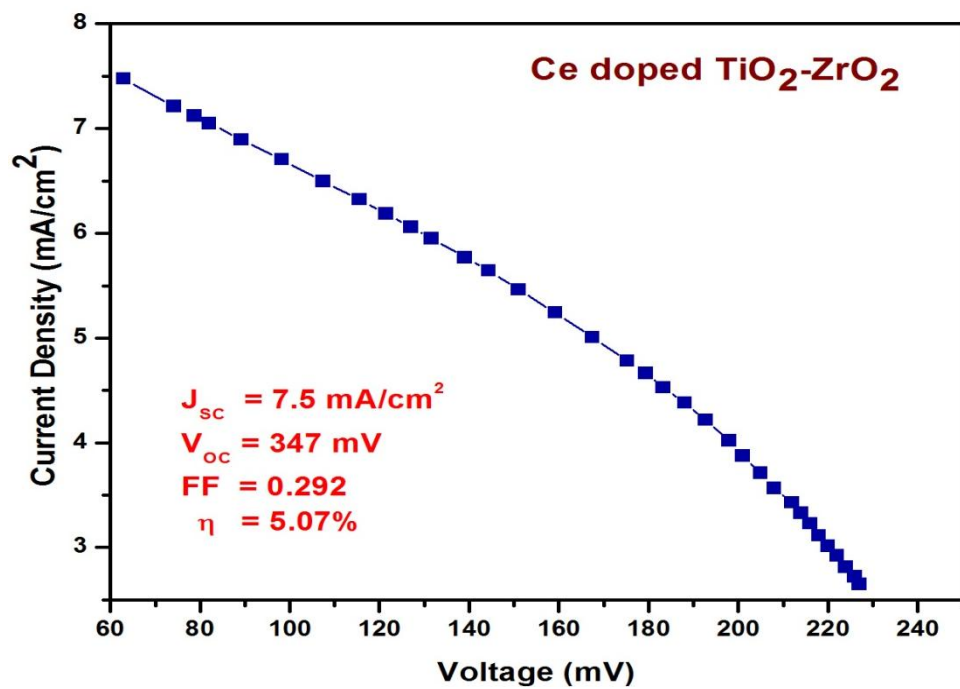


Figure 8.20 I-V curve of DSSC prepared using Cerium doped TiO₂-ZrO₂

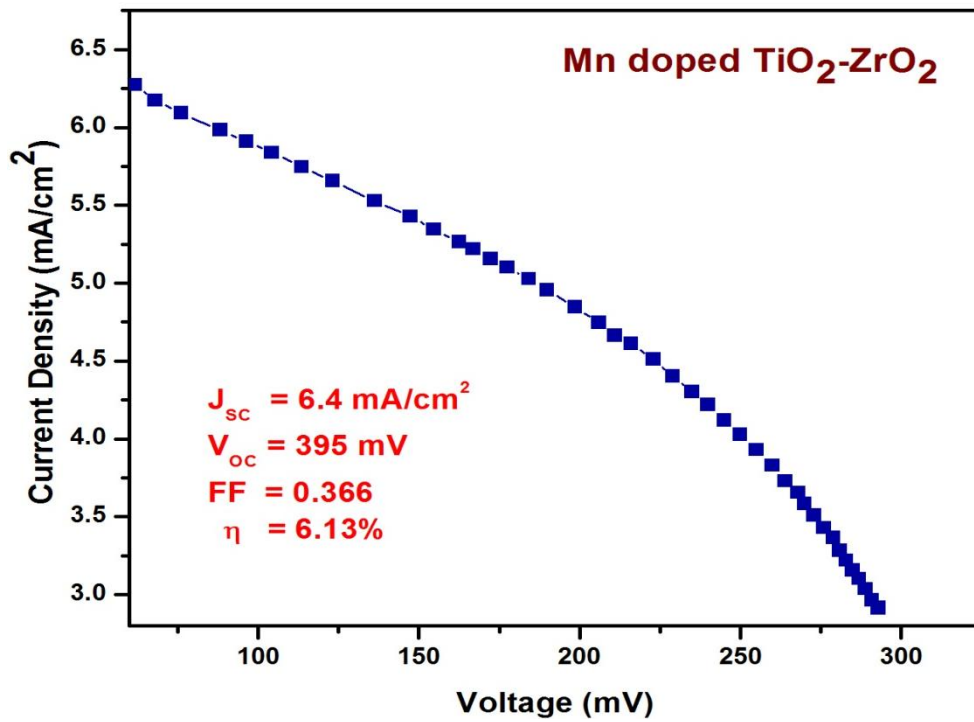


Figure 8.21 I-V curve of DSSC prepared using Manganese doped TiO₂-ZrO₂

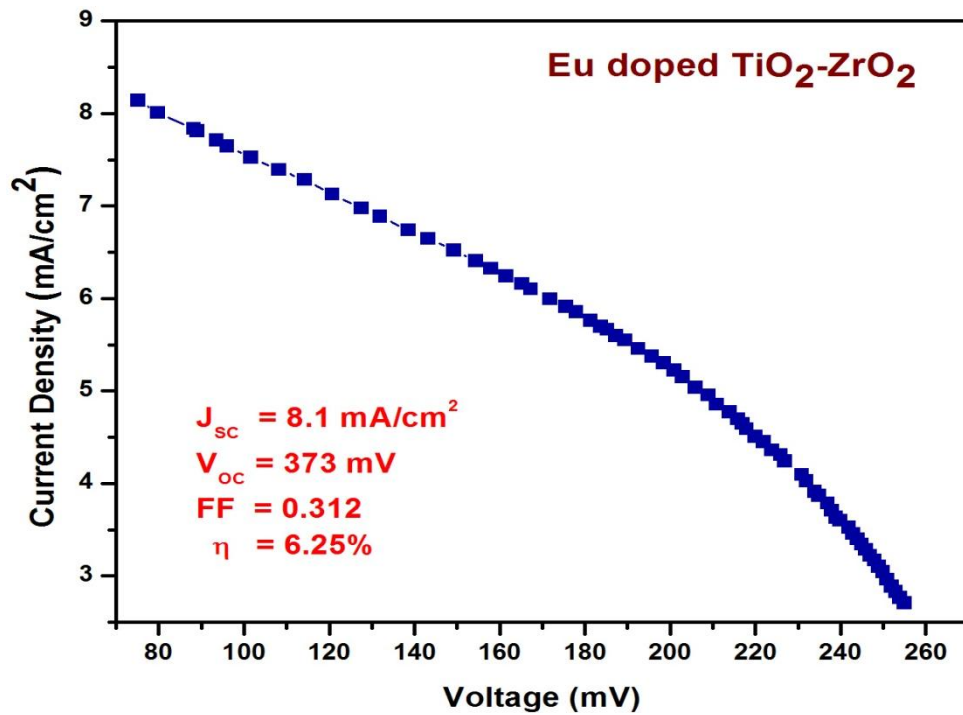


Figure 8.22 I-V curve of DSSC prepared using Europium doped TiO₂-ZrO₂

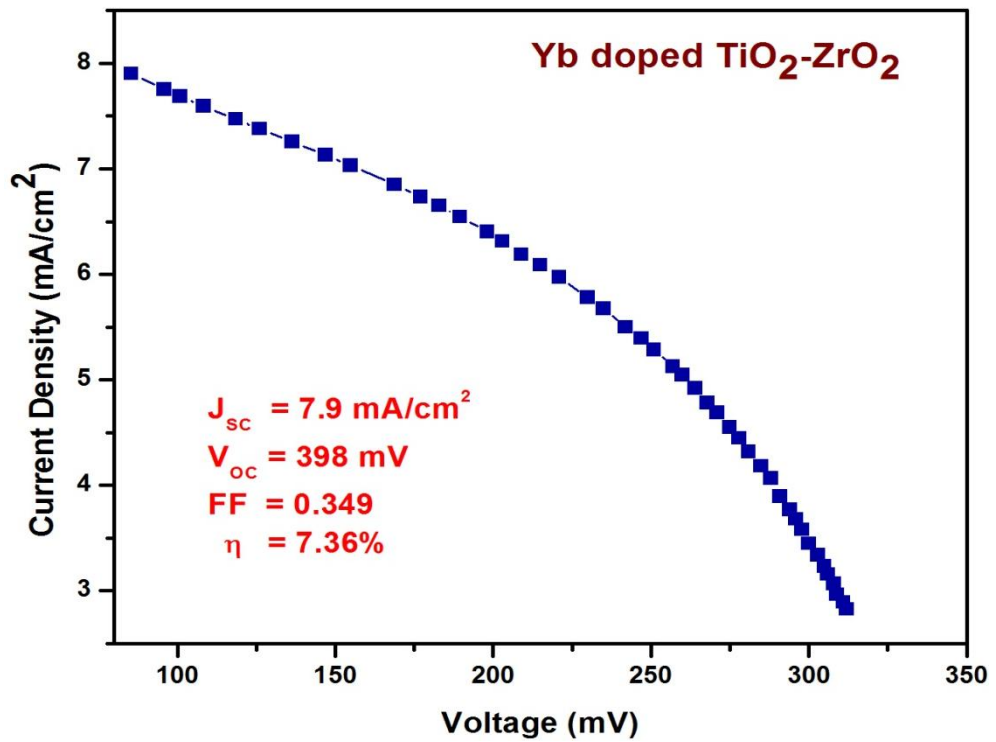


Figure 8.23 I-V curve of DSSC prepared using Ytterbium doped TiO₂-ZrO₂

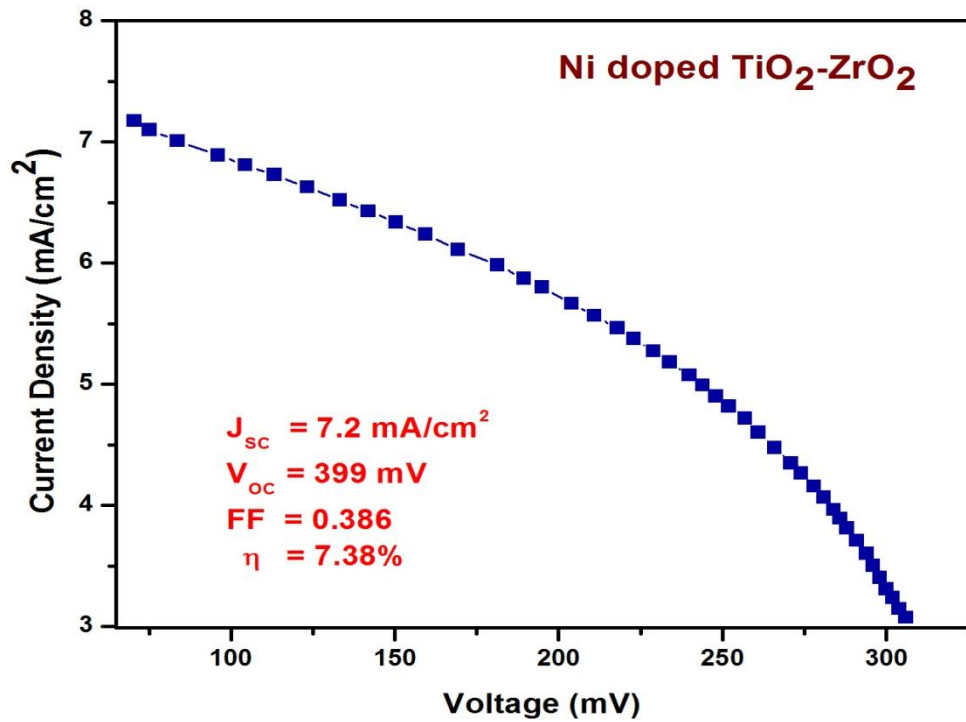


Figure 8.24 I-V curve of DSSC prepared using Nickel doped TiO₂-ZrO₂

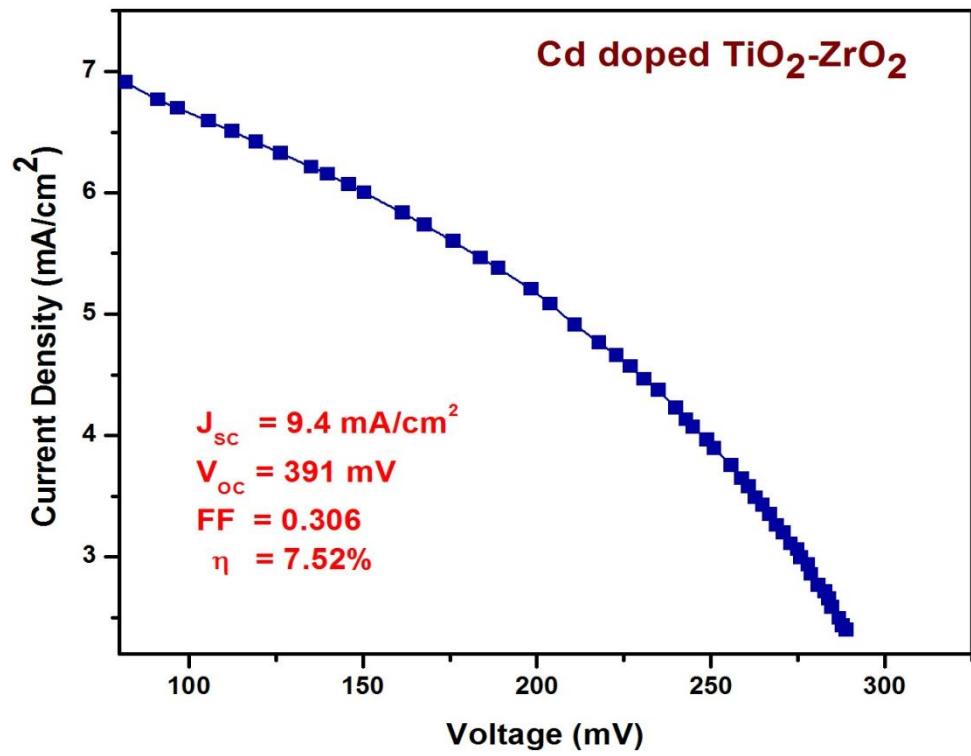


Figure 8.25 I-V curve of DSSC prepared using Cadmium doped TiO₂-ZrO₂

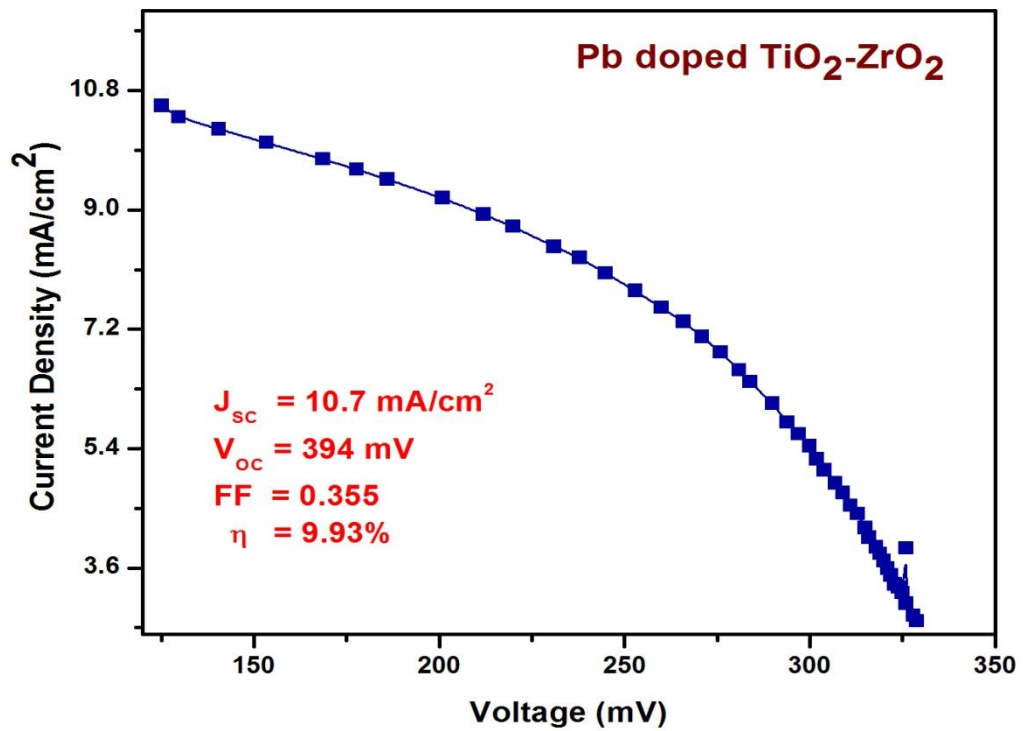


Figure 8.26 I-V curve of DSSC prepared using Lead doped TiO₂-ZrO₂

Table 8.2 Efficiency parameters of DSSC prepared using metal doped TiO₂-ZrO₂

Sample	Area Cm ²	R _{shunt} (Ω)	R _{series} (Ω)	J _{sc} mA/cm ²	V _{oc} mV	FF	η %
Mg doped TiO ₂ -ZrO ₂	1.00	0.058	0.044	3.9	282	0.295	2.15
La doped TiO ₂ -ZrO ₂	1.21	0.052	0.039	4.3	346	0.216	2.26
Cu doped TiO ₂ -ZrO ₂	1.21	0.113	0.080	3.5	383	0.258	2.31
Er doped TiO ₂ -ZrO ₂	1.26	0.099	0.033	4.8	382	0.287	3.52
Al doped TiO ₂ -ZrO ₂	1.21	0.153	0.048	4.6	387	0.327	3.88
Fe doped TiO ₂ -ZrO ₂	1.32	0.063	0.017	5.7	351	0.292	3.88
Zn doped TiO ₂ -ZrO ₂	1.00	0.058	0.034	5.9	369	0.312	4.58
Ce doped TiO ₂ -ZrO ₂	1.10	0.040	0.017	7.5	347	0.292	5.07
Mn doped TiO ₂ -ZrO ₂	1.10	0.085	0.029	6.4	395	0.366	6.13
Eu doped TiO ₂ -ZrO ₂	1.00	0.036	0.012	8.1	373	0.312	6.25
Yb doped TiO ₂ -ZrO ₂	1.20	0.061	0.015	7.9	398	0.349	7.36
Ni doped TiO ₂ -ZrO ₂	1.10	0.084	0.022	7.2	399	0.386	7.38
Cd doped TiO ₂ -ZrO ₂	1.20	0.057	0.014	9.4	391	0.306	7.52
Pb doped TiO ₂ -ZrO ₂	1.32	0.042	0.008	10.7	394	0.355	9.94

The results indicate that doping of metal into $\text{TiO}_2\text{-ZrO}_2$ increases the efficiency of DSSC compared to that of undoped $\text{TiO}_2\text{-ZrO}_2$. The I-V characteristics of DSSC prepared using metal doped $\text{TiO}_2\text{-ZrO}_2$ are better than undoped $\text{TiO}_2\text{-ZrO}_2$ in terms of all the parameters. This can be attributed to the improved conductivity of $\text{TiO}_2\text{-ZrO}_2$ due to metal doping, apart from other reasons.

It has been reported that the I-V curve deviate from its ideal behavior if the resistance present in DSSC is very high. The main components of series resistance include sheet resistance of the conducting plate, resistance of contacts and the resistance of photo electrode material. The shunt resistance is mainly caused due to leakage current through the cell caused by impurities or defects in the manufacturing process. The value of series resistance is decreased in DSSC prepared using metal doped $\text{TiO}_2\text{-ZrO}_2$. The lowest series resistance has been observed for DSSC prepared using Pb doped $\text{TiO}_2\text{-ZrO}_2$, which has been found to have the highest efficiency. Since the series resistance is lower, it indicates improvement in the quality of the photo cathode material, which is obviously due to doping.

There are several other structural and optical parameters which affect the efficiency of DSSC. The crystallite size of metal doped $\text{TiO}_2\text{-ZrO}_2$ is smaller than undoped $\text{TiO}_2\text{-ZrO}_2$ samples. Hence the decrease in crystallite size of the material also improves the performance. This can be attributed to increase in surface area on account of lower crystallite size which results into higher amount of dye being adsorbed on the film.

The Anatase content in almost all the metal doped samples is higher than 70%. Samples doped with Lanthanum, Cadmium, Ytterbium and Lead have 100%

Anatase phase of TiO_2 , which can be one of the major reasons for the enhanced efficiency of DSSC made out of these material.

The higher efficiencies of the cells can be explained as a consequence of reduced recombination, which results in an increase of electron density in metal doped TiO_2 - ZrO_2 layer. The metal doping is likely to reduce the recombination of electrons with oxidizing species like triiodide ions in the electrolyte as well as the dye.

It has been reported that electron conductivity in TiO_2 and ZrO_2 is comparatively low resulting in slow response of the photocurrent [26]. However, the metal doping introduces new energy levels below the conduction band, improves the conductivity and as a consequence, the response of photocurrent. The introduction of these energy levels provides additional channels for collection of electrons at the working electrode. This can result into higher photocurrent density. The metal ions may act as a deterrent between TiO_2 - ZrO_2 and dye interface and inhibited the recombination process. This schematic explanation is proposed in figure 8.27.

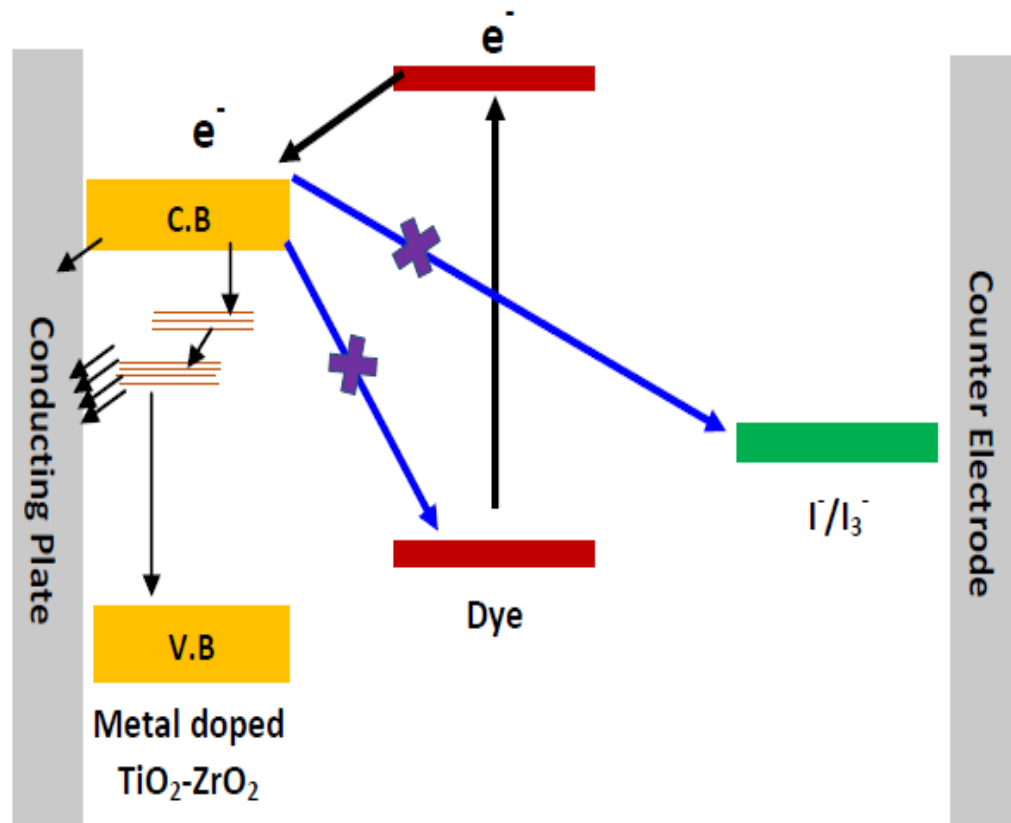


Figure 8.27 Charge transportation process in metal doped $\text{TiO}_2\text{-ZrO}_2$ nanocomposite

DSSC prepared using Pb doped $\text{TiO}_2\text{-ZrO}_2$ exhibits highest short current density ($J_{\text{SC}} = 10.7 \text{ mA/cm}^2$) and finally the highest power conversion efficiency ($\eta = 9.94\%$). These results are encouraging as the highest reported efficiency of DSSC is around 11%.

8.6 Performance of Dye Sensitized Solar Cell fabricated using co-doped TiO₂-ZrO₂

The efficiency of DSSC improves by metal doping in TiO₂-ZrO₂ mixed oxides. An attempt was made to study the performance of these oxides by co-doping of the already studied single doped metal ions. The pairing was done by a combination of transition/alkaline earth and rare earth metal ions. The alkaline/transition metal ions taken were Copper, Aluminium, Zinc and Manganese in that order, as DSSC's prepared by the single doped samples of these same metal ions give efficiencies in the same order in increasing progression. The two rare earth co-dopants taken are Cerium and Europium, which are easily available.

These metals were doped together in TiO₂-ZrO₂ and DSSC's were prepared by applying them as the photo electrode material. Its power conversion efficiency was studied. The J-V characteristics of DSSCs prepared using co-doped TiO₂-ZrO₂ are shown in figures 8.28 to 8.35. The calculated efficiency parameters of these cells are summarized in Table 8.3.

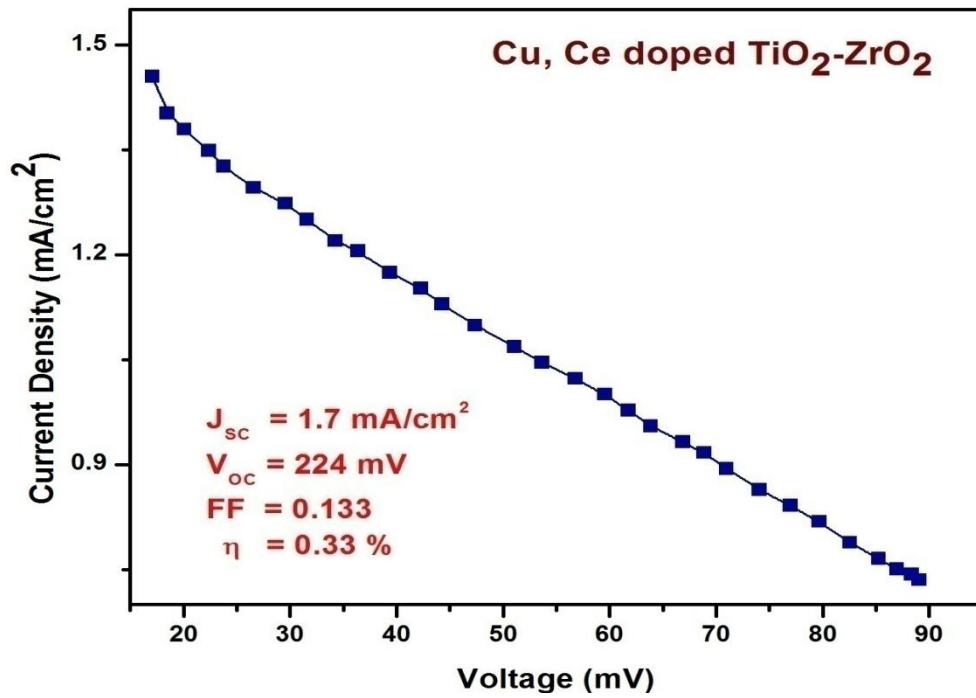


Figure 8.28 J-V curve of DSSC prepared using TiO₂-ZrO₂ doped with Copper and Cerium

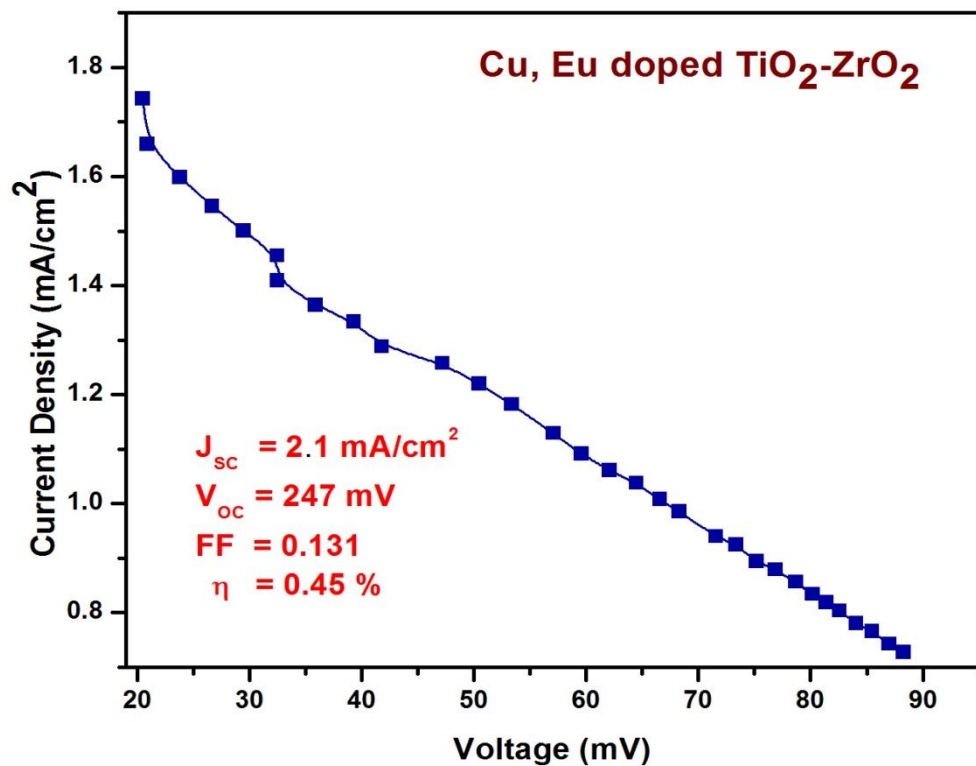


Figure 8.29 J-V curve of DSSC prepared using TiO₂-ZrO₂ doped with Copper and Europium

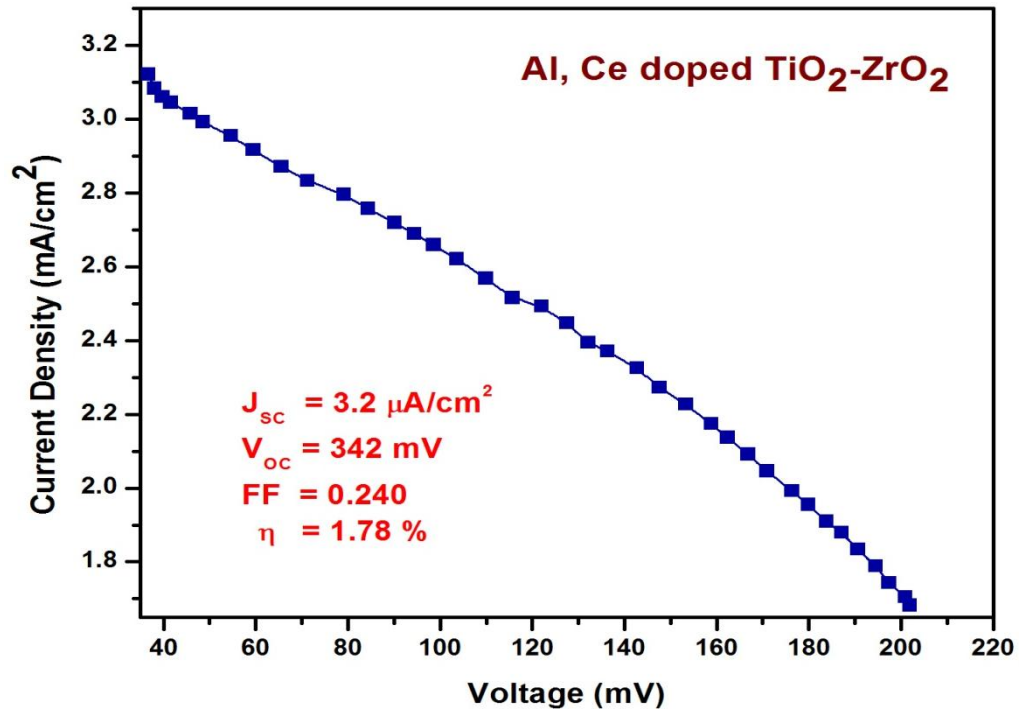


Figure 8.30 J-V curve of DSSC prepared using TiO₂-ZrO₂doped with Aluminium and Cerium

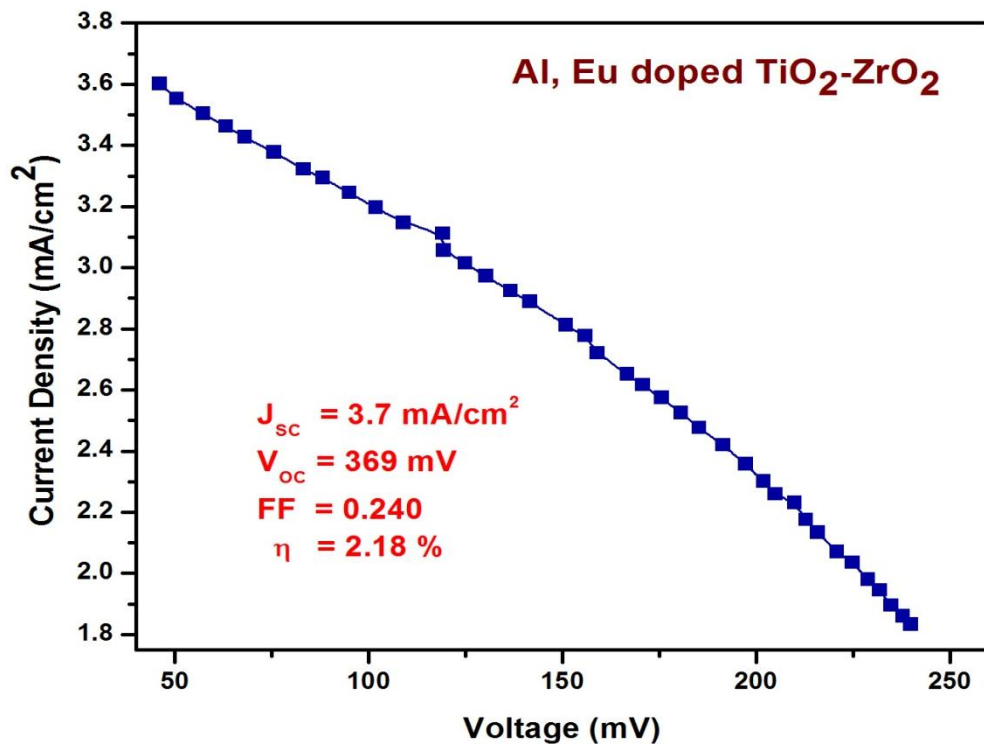


Figure 8.31 J-V curve of DSSC prepared using TiO₂-ZrO₂ doped with Aluminium and Europium

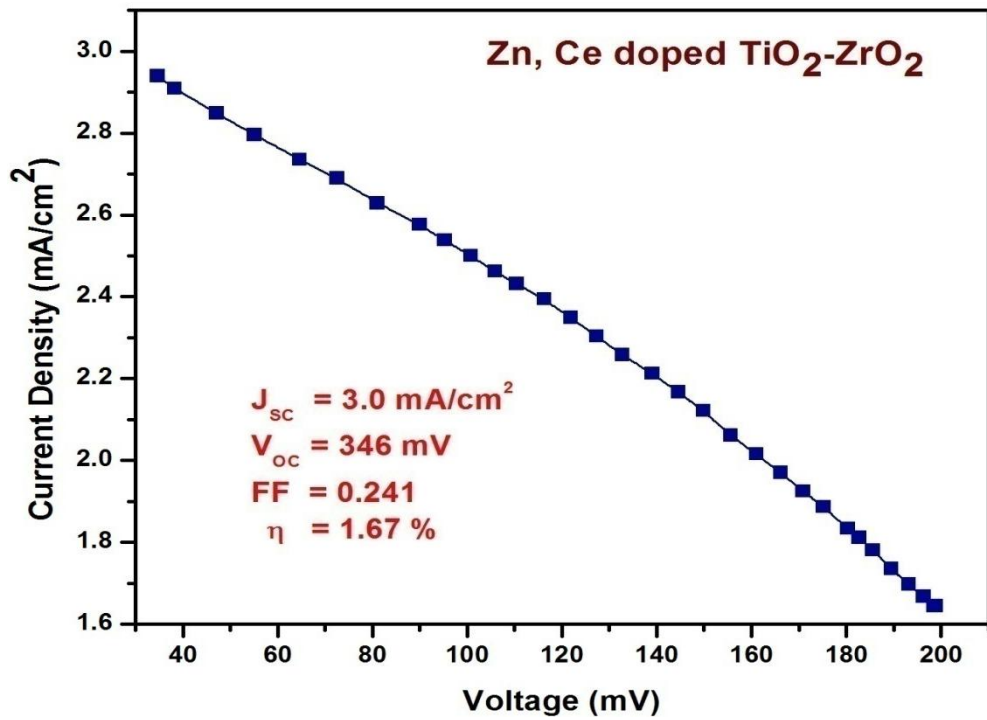


Figure 8.32 J-V curve of DSSC prepared using TiO₂-ZrO₂ doped with Zinc and Cerium

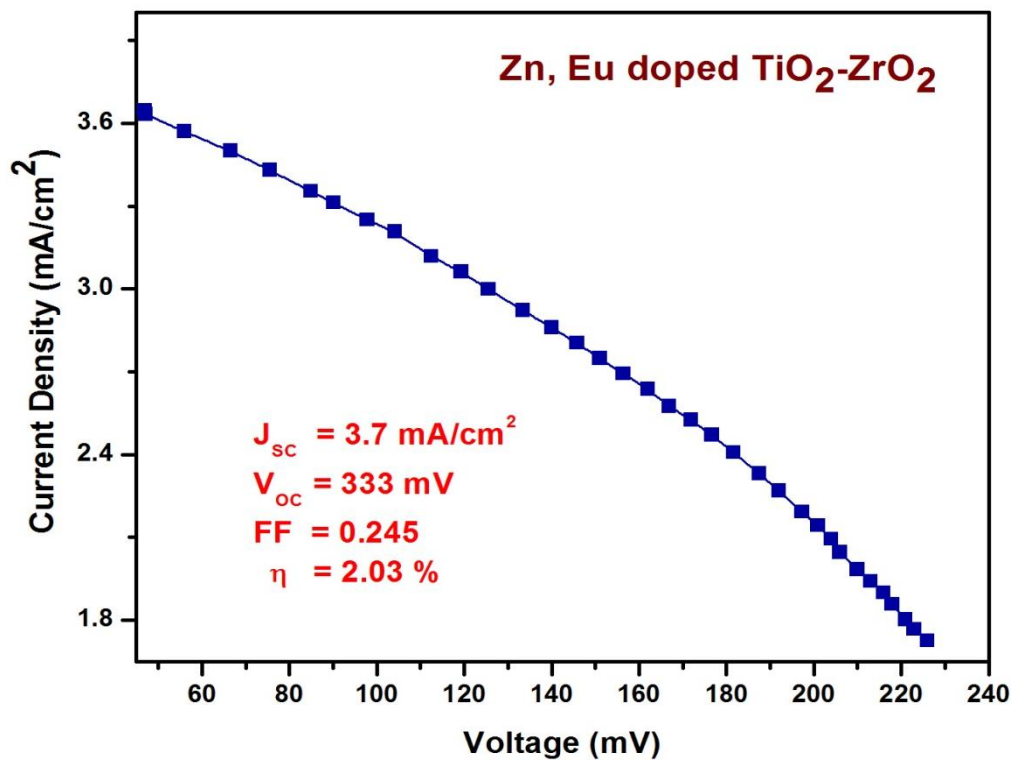


Figure 8.33 J-V curve of DSSC prepared using TiO₂-ZrO₂ doped with Zinc and Europium

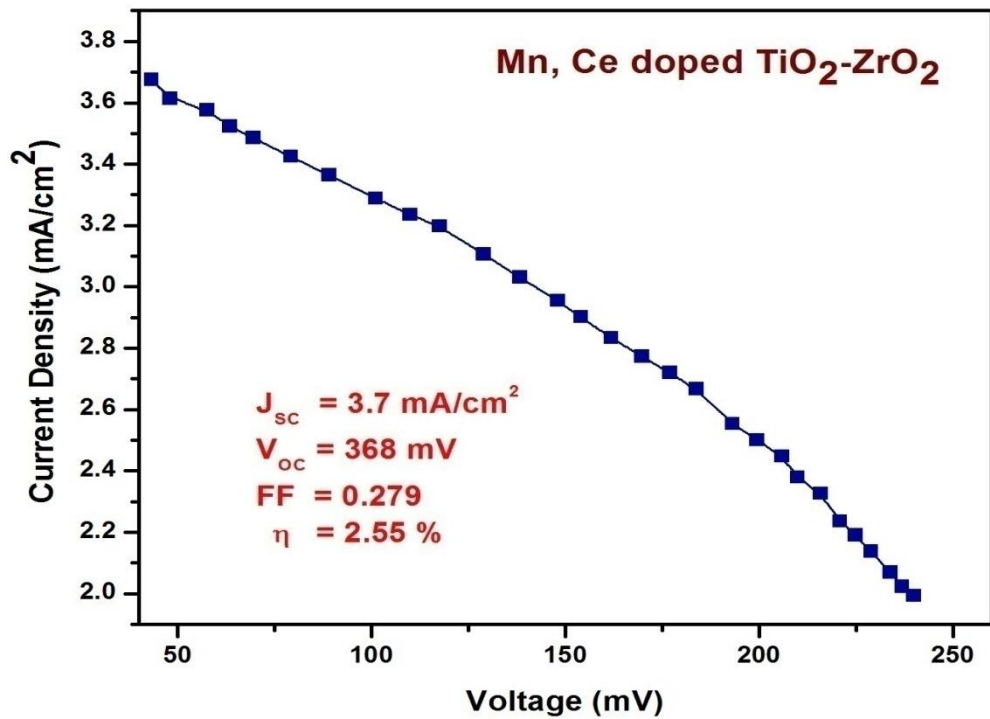


Figure 8.34 J-V curve of DSSC prepared using TiO₂-ZrO₂ doped with Manganese and Cerium

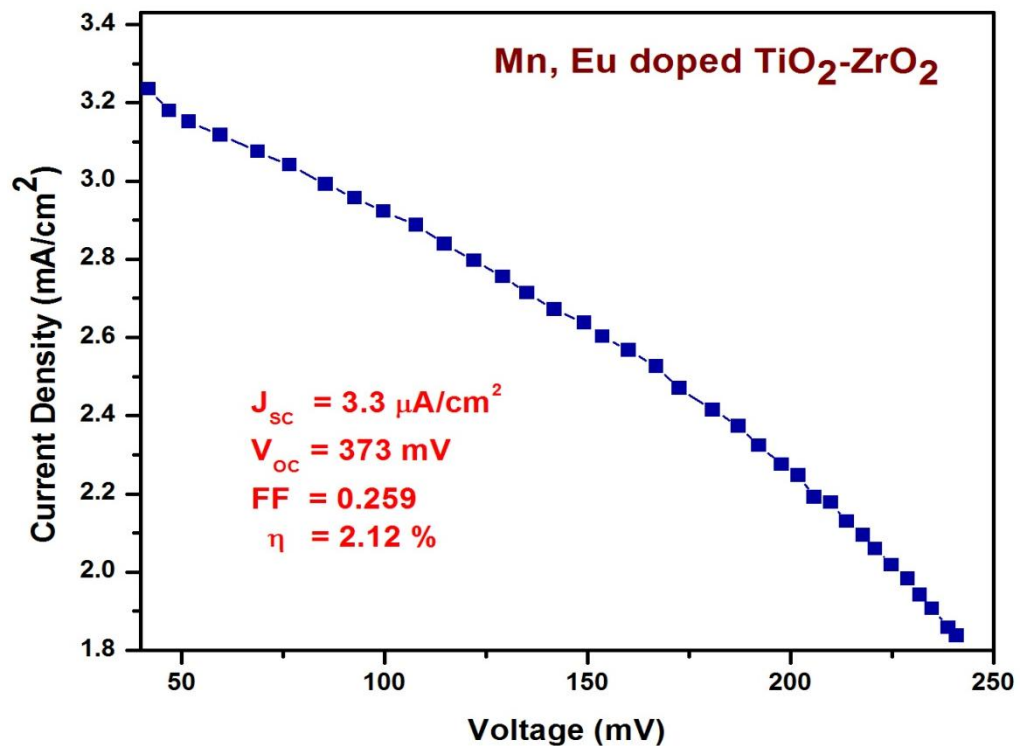


Figure 8.35 J-V curve of DSSC prepared using TiO₂-ZrO₂ doped with Manganese and Europium

Table 8.3 Efficiency parameters of DSSC prepared using metal doped TiO₂-ZrO₂nanocomposites

Sample	Area Cm ²	R _{shunt} (Ω)	R _{series} (Ω)	J _{sc} mA/cm ²	V _{oc} mV	FF	η %
Cu, Ce doped TZ	1.32	-	-	1.7	224	0.133	0.33
Cu, Eu doped TZ	1.15	-	-	2.1	247	0.131	0.45
Al, Ce doped TZ	1.32	0.077	0.055	3.2	342	0.240	1.78
Al, Eu doped TZ	1.43	0.087	0.051	3.7	369	0.240	2.18
Zn, Ce doped TZ	1.32	0.108	0.076	3.0	346	0.241	1.67
Zn, Eu doped TZ	1.44	0.097	0.041	3.7	333	0.245	2.03
Mn, Ce doped TZ	1.32	0.110	0.056	3.7	368	0.279	2.55
Mn, Eu doped TZ	1.44	0.107	0.059	3.3	373	0.259	2.12

Comparing the efficiencies with those of the single doped material of the same ions, the efficiencies of DSSC's made out of co-doped samples fall much short, which puts a question mark on the effectiveness of the co-doped material. The reason for this may be the further introduction of additional energy levels due to the co-dopant, where electrons get trapped. These energy states provide additional path for recombination of electrons back to the valence band of the photocathode material. Hence, more electrons get recombined rather than getting collected at the

working electrode, decreasing the current density. This is schematically proposed in figure 8.36

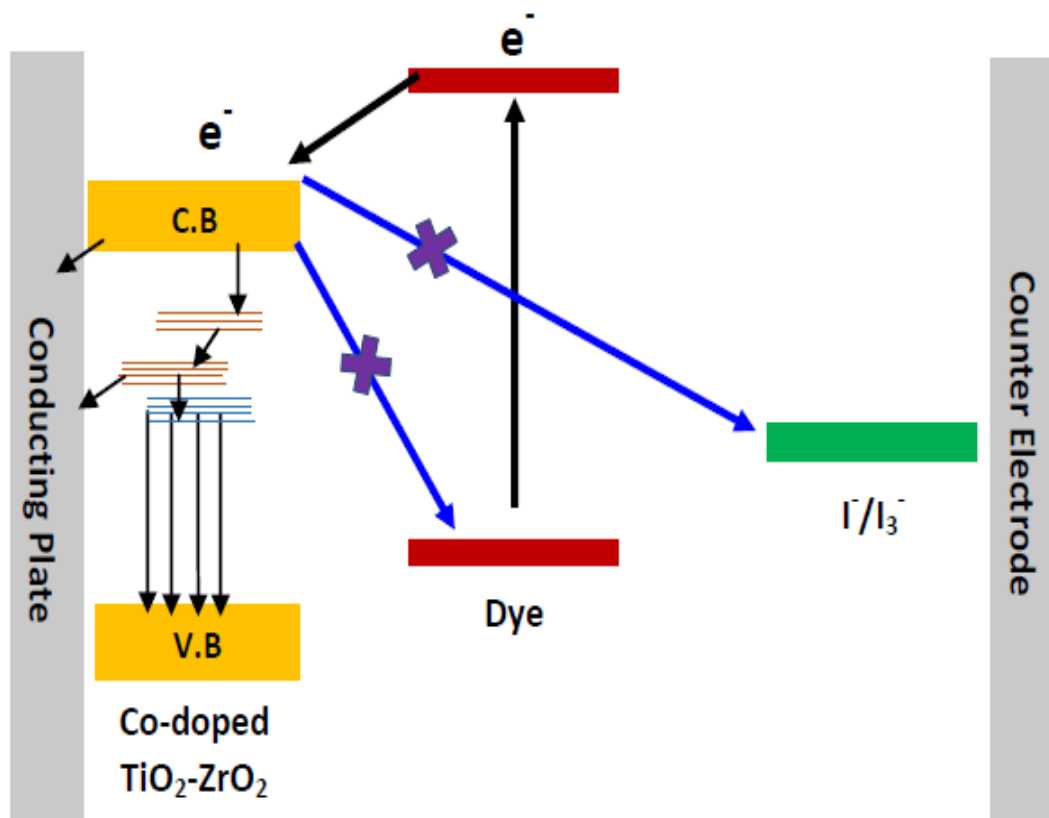


Figure 8.36 Charge transportation process in co-doped $\text{TiO}_2\text{-ZrO}_2$ nanocomposite

8.7 Conclusion

Dye Sensitized Solar Cells were fabricated using simple technique and inexpensive components. The cells prepared using un-doped $\text{TiO}_2\text{-ZrO}_2$ mixed oxides give a highest efficiency of 5.97%. Further increment in efficiency has been observed for DSSC prepared using metal doped $\text{TiO}_2\text{-ZrO}_2$ samples. The improvement in structural properties of $\text{TiO}_2\text{-ZrO}_2$ due to doping may be responsible for this enhancement in efficiency. The presence of metal ions may have inhibited the recombination process. The highest efficiency of 9.94% has been recorded for the DSSC prepared using Lead doped $\text{TiO}_2\text{-ZrO}_2$. Two metals were doped together in $\text{TiO}_2\text{-ZrO}_2$ in an attempt to study the effect of co-doping on the efficiency. The efficiency of DSSC prepared using co-doped samples were found to be much lower than the efficiency of single metal doped samples. A highest efficiency of only 2.55% has been observed for the sample co-doped with Manganese and Cerium. This is in spite of the fact that the Anatase content of these samples is quite high. Hence, the lower efficiencies may be attributed to the generation of new trap states below the conduction band of $\text{TiO}_2\text{-ZrO}_2$. The electrons are trapped in these energy levels rather than reaching the conducting plate. The trap states also provide alternate path for recombination of the electrons in the valence band.

References

- [1] B. O'Regan, M. Gratzel, *Nature* 1991, 353, 737.
- [2] M. Gratzel, *Nature* 2001, 414, 338.
- [3] N. J. Podraza, C. Chen, D. Sainju, O. Ezekoye, M. W. Horn, C. R. Wronski, R. W. Collins, R. W. Mater. Res. Soc. Symp. Proc. 2005, 865, 273.
- [4] W. J. Lee, E. Ramasamy, D. Y. Lee, B. K. Min, J. S. Song, *Proc. SPIE-Int. Soc. Opt. Eng.* 2006, 413.
- [5] Y. Saito, S. Kambe, T. Kitamura, Y. Wada, S. Yanagida, *Sol. Energy Mater. Sol. Cells* 2004, 83, 1.
- [6] Z. S. Wang, H. Kawauchi, T. Kashima, H. Arakawa, *Coord. Chem. Rev.* 2004, 248, 1381.
- [7] M. K. Nazeeruddin, P. Pechy, T. Renouard, S. M. Zakeeruddin, R. Humphry-Baker, P. Comte, P. Liska, L. Cevey, E. Costa, V. Shklover, L. Spiccia, G. B. Deacon, C. A. Bignozzi, M. Graetzel, *J. Am. Chem. Soc.* 2001, 123, 1613.
- [8] K. Hara, T. Nishikawa, M. Kurashige, H. Kawauchi, T. Kashima, K. Sayama, K. Aika, H. Arakawa, *Sol. Energy Mater. Sol. Cells* 2005, 85, 21.
- [9] X. Fang, T. Ma, G. Guan, M. Akiyama, T. Kida, E. Abe, *J. Electroanal. Chem.* 2004, 570, 257.
- [10] N.G. Park, G. Schlichthorl, J. van de Lagemaat, H.M. Cheong, A. Mascarenhas, A.J. Frank, *J. Phys. Chem. B.* 1999, 103, 3308–3314.
- [11] S. Anderson, *Nature* 1979, 280, 571–573.
- [12] M. Dare Edwards, *Faraday Discuss. Chem. Soc.* 1980, 70, 285–298.
- [13] S. Michal, C. Julius, *Acta Electrotechnica et Informatica* 2010, 10, 78–81
- [14] H. Gerischer, H. Tributsch, *B. Bunsen. Phys. Chem.* 1968, 72, 437–445.
- [15] H. Tributsch, H. Gerischer, *B. Bunsen. Phys. Chem.* 1969, 73, 251–260.

- [16] A.S. Polo, M.K. Itokazu, N.Y. Murakami Iha, *Coord. Chem. Rev.* 2004, 248, 1343-1361.
- [17] K. Hara, *Sol. Energy Mater. Sol. Cells* 2001, 70, 151–161.
- [18] N. Vlachopoulos, P. Liska, J. Augustynski, M. Gratzel, *J. Am. Chem. Soc.* 1988, 110, 1216–1220.
- [19] N. Papageorgiou, W.F. Maier, M. Grätzel, *J. Electrochem. Soc.* 1997, 144, 876.
- [20] K. Imoto, K. Takahashi, T. Yamaguchi, T. Komura, J. Nakamura, K. Murata, *Sol. Energy Mater. Sol. Cells* 2003, 79, 459.
- [21] K. Suzuki, M. Yamaguchi, M. Kumagai, S. Yanagida, *Chem. Lett.* 2003, 32, 28.
- [22] Keithley Application Note Series, Making I-V and C-V Measurements on Solar/Photovoltaic Cells Using the Model 4200-SCS Semiconductor Characterization System, 2876
- [23] Umass Boston, ChemAdvanced Inorganic Chemistry Laboratory, 371
- [24] N.G. Park, J. van de Lagemaat, A.J. Frank, *J. Phys. Chem. B.* 2000, 104, 8989–8994.
- [25] Bing Tan and Yiying Wu, *J. Phys. Chem. B* 2006, 110, 15932-15938
- [26] Kohjiro Hara and Hironori Arakawa, *Handbook of Photovoltaic Science and Engineering*. Edited by A. Luque and S. Hegedus, 2003 John Wiley & Sons, Ltd.